Computational and Applied Mathematics (2022) 41:289
https://doi.org/10.1007/s40314-022-01990-4

# Analysis and dynamics of a mathematical model to predict unreported cases of COVID-19 epidemic in Morocco

**Abdelouahed Alla Hamou[1] · Rando R. Q. Rasul[2] · Zakia Hammouch[3,5,6] · Necati Özdemir[4]**

Received: 20 February 2022 / Revised: 17 July 2022 / Accepted: 25 July 2022 /
Published online: 20 August 2022


**Abstract**
In December 2019, in Wuhan, China, a new disease was detected, and the virus easily spread throughout other nations. March 2, 2020, Morocco announced 1st infection of coronavirus. Morocco verified a total of 653,286 cases, 582,692 recovered, 60,579 active case, and 10,015 as confirmatory fatalities, as of 4 August 2021. The objective of this article is to study the mathematical modeling of undetected cases of the novel coronavirus in Morocco. The model is shown to have disease-free and an endemic equilibrium point. We have discussed the local and global stability of these equilibria. The parameters of the model and undiscovered instances of COVID-19 were assessed by the least squares approach in Morocco and have been eliminated. We utilized a Matlab tool to show developments in undiscovered instances in Morocco and to validate predicted outcomes. Like results, until August 4, 2021, the total number of infected cases of COVID-19 in Morocco is 24,663,240, including 653,286 confirmed cases, against 24,009,954 undetected. Further, our approach gives a good approximation of the actual COVID-19 data from Morocco and will be used to estimate the undetected cases of

Communicated by Rafael Villanueva.

✉ Zakia Hammouch
hammouch_zakia@tdmu.edu.vn

Abdelouahed Alla Hamou
abdelouahed.allahamou@gmail.com

Rando R. Q. Rasul
rando.qadir@univsul.edu.iq

1 Faculty of Sciences Dhar Al Mahraz, Sidi Mohamed Ben Abdellah University, B.P. 1796, 30000 Fez, Morocco

2 Department of Mathematical Sciences, College of Basic Education, University of Sulaimani, Sulaimani, Kurdistan Region, Iraq

3 Division of Applied Mathematics, Thu Dau Mot University, Thu Dau Mot, Binh Duong, Vietnam

4 Department of Mathematics, Faculty of Arts and Sciences, Balıkesir University, Balıkesir, Turkey

5 Department of Medical Research, China Medical University Hospital, Taichung, Taiwan

6 Department of Sciences, ENS Moulay Ismail University of Meknes, Meknes, Morocco

COVID-19 in other countries of the world and to study other pandemics that have the same nature of spread as COVID-19.

**Keywords** Unreported COVID-19 cases · SARS-CoV-2 · SEIRD epidemic model · Epidemiology · Least squares method · Parameter estimation

**Mathematics Subject Classification** 65D05 · 65R20 · 26A33 · 93E24

## 1 Introduction

In December 2019, the Corona virus appeared in China, specifically in Wuhan, Hubei province (Cohen and Normile 2020), where it then spread throughout the world to become a global epidemic. Among these countries that have been greatly affected by the virus, we find Morocco. As of August 4, 653,286 infected cases have been recorded, including 10,015 deaths, and nearly 582,692 have recovered from the virus. The number of infected people in the world at the same date reached nearly 201 million. After the spread of this virus, researchers and laboratories analyzed and studied the evolution of this virus, as some of them relied on laboratory results and some on theoretical studies using real data. Cases confirmed by governments, laboratories or the World Health Organization only are the result of positive tests, but there are a group of cases infected with the virus, but they are not discovered, either because the infected person did not feel the symptoms of this virus or that he did not have the possibility to go to the hospital or that the symptoms he feels are considered normal And you do not need tests, just wait at home until he recovers. The goal of this study is to determine the number of infected and recovered cases and death due to the virus, but it was not discovered (undetected or unreported), and we will also approximate and predict the evolution of the virus based on the real data of this virus. Among the most famous of these mathematical methods used, we find the epidemiological models. Among the most famous epidemiological models that have been used to model several epidemics, including COVID-19, are basic SIR (susceptible–infectious–recovered) and SEIR (susceptible–exposed–infectious–recovered) models (Korobeinikov 2009). There are many researches that have been carried out in this regard. An updated COVID-19 SIR model is assessed in Calafiore et al. (2020) from Italy. In Watve et al. (2021) the classical SIR model and its derivatives is used to predict the outbreak of COVID-19 in Isfahan province of Iran. A susceptible–infected–recovered dynamics of COVID-19 and economic impact is proposed in Toda (2020). An epidemiological model with isolation and quarantine is proposed in paper Hamou et al. (2021b) the effect and importance of fractional derivative is shown in Alla Hamou et al. (2020) and Hamou et al. (2021a) by model predictions using the Least Squares method. Other work on COVID-19 can be found in Simoy and Aparicio (2022), Yang et al. (2021), Perakis et al. (2022) and Haque et al. (2022). When an individual is a carrier of the virus, she may not feel any symptoms, which causes her to transmit the virus, so are other infected cases, despite their feeling of mild or moderate symptoms, but they do not go away. hospital to do the tests, some of them are recovering and some of them die from the virus, these cases are said to be undetected. They are the ones that cause the virus to spread rapidly

The aim of this study is to determine the number of true cases infected with the virus, that is, not detected and not confirmed by governments. We will determine cases of infection, death and undetected cures using a modified version of the SEIRD epidemiological model and actual data from COVID-19, and we apply our model to the case of Morocco. Some studies

interested in determining the number of undetected cases of COVID-19 using epidemiological models. Rippinger et al. (2021) determined the impact of detection probabilities, using the fractions of unreported and reported cases of COVID-19 during an epidemic wave in Austria. A study estimated the number of cases in China in the period from January 10 to January 23, 2020 (Li et al. 2020), it found that 86% of all infections were undetected. The best-fitting model parameters were identified by log likelihood. A similar mathematical model has been used by Pei et al. (2018) to predict the transmission of influenza in the USA. Based on 50,006 reported cases (Huo et al. 2021) determined that among 64,454 infected, there are 14,448 undetected in Wuhan, China with a detection rate of 77.58%, Salje et al. (2020) have estimated the impact of confinement and the current immunity of the French population, they found that 2.9% of infected people are hospitalized and 0.5% of infected people die.

A mathematical model named SIPHERD is presented in Mahajan et al. (2020), this model gives an estimate of detected and undetected cases of infection, and also asymptomatic or symptomatic cases of COVID-19 in United States of America, The researcher estimates in Mahajan et al. (2021) the undiscovered symptomatic COVID 19 patients, utilizing an epidemic, symptomatic, unadulterated unaffected, and three-category disease transmitters approach, in the USA. All these studies do not offer the prediction of undetected recovered cases and undetected deaths.

Throughout this work we develop an infectious system, entitled SEIRDB, for the COVID-19 epidemics, and use it to predict the number of detected and undetected patients in Morocco, therefore our aim is to provide a comprehensive model to calculate the number of incidents undetected infected and recovered and dead.

The paper is organized as follows. In Sect. 2, the mathematical model is formulated. Well-posedness of the model is studied in Sect. 3. The basic reproduction number and the equilibria are given in Sect. 4. Some discussions on the local and global stability of equilibria are given in Sects. 5 and 6 respectively. Simulation and calibration results are presented in Sect. 7. Finally, the present work is concluded in Sect. 8.

## 2 Interpretation of the model

The purpose of this article is to find out the percentage of undiscovered infected patients, undetected recovery, and undetected deaths of COVID-19 in Morocco, using an ecological modelling of the form of SEIRD. This model consists of two groups, one of the detected cases and the other of the undetected cases. The studied population must be divided into nine compartments, susceptible ($S$), exposed ($E$), infected detected ($I_d$) (or isolated or hospitalized), recovered detected ($R_d$), death detected ($D_d$), infected undetected ($I_u$), recovered undetected ($R_u$), undetected death ($D_u$), detected death ($D_d$) and buried ($B$).

The transmission of COVID-19 is not only due to contact with undetected infected in the community ($I_u$), but also with detected and isolated patients ($I_d$) and also with improper handling of undetected dead bodies ($D_d$). This last type of transmission has been discussed and confirmed in some papers, for example, in Gabbrielli et al. (2021) researchers have found that SARS-CoV-2 can be transmitted from people who have died for a certain period after death as well as the viral genome of SARS-CoV-2 can persist in tissues for more than 30 days. For more discussions on this topic, see Sriwijitalai and Wiwanitkit (2020), Gabbrielli et al. (2021), Zapor (2020) and Yaacoub (2020).

Then, the instantaneous rate of change on the number of individuals susceptible can be expressed as

$$\frac{\mathrm{d}S}{\mathrm{d}t} = -\frac{(\beta_{\mathrm{u}} I_{\mathrm{u}} + \beta_{\mathrm{d}} I_{\mathrm{d}} + q D_{\mathrm{u}})S}{N}, \tag{1}$$

where $\beta_{\mathrm{u}}$ is the transmission rate in the community , $\beta_{\mathrm{d}}$ is the transmission rate in hospitals or anywhere to isolate patients and $q$ is the transmission rate at funerals by touching dead bodies. The incubation period of COVID-19 for detected and undetected cases is $1/\sigma$. Then the instantaneous rate of change on the number of individuals exposed can be expressed as

$$\frac{\mathrm{d}E}{\mathrm{d}t} = \frac{(\beta_{\mathrm{u}} I_{\mathrm{u}} + \beta_{\mathrm{d}} I_{\mathrm{d}} + q D_{\mathrm{u}})S}{N} - \tau\sigma E - (1-\tau)\sigma E, \tag{2}$$

where $\tau$ is the proportion of individuals exposed to the virus is infected and undetected. Likewise infectious period of detected and undetected cases are $1/\gamma_{\mathrm{d}}$ and $1/\gamma_{\mathrm{u}}$ respectively. Detected and undetected cases die at rates $\mu_{\mathrm{d}}$ and $\mu_{\mathrm{u}}$ respectively, it is normal for $\mu_{\mathrm{d}}$ to be smaller than $\mu_{\mathrm{u}}$, because the detected cases are subject to hospital care and artificial respiration, etc. Some cases undetected can be confirmed with PCR tests (Zhu et al. 2020; Watson et al. 2020) and move to the detected cases at rate $\delta$, then the instantaneous rates of change on the number of individuals infected are given by

$$\frac{\mathrm{d}I_{\mathrm{u}}}{\mathrm{d}t} = \tau\sigma E - (\mu_{\mathrm{u}} + \delta + \gamma_{\mathrm{u}})I_{\mathrm{u}} \quad \text{and} \quad \frac{\mathrm{d}I_{\mathrm{d}}}{\mathrm{d}t} = (1-\tau)\sigma E + \delta I_{\mathrm{u}} - (\mu_{\mathrm{d}} + \gamma_{\mathrm{d}})I_{\mathrm{d}}, \tag{3}$$

and the then the instantaneous rates of change on the number of individuals recovered are given by

$$\frac{\mathrm{d}R_{\mathrm{u}}}{\mathrm{d}t} = \gamma_{\mathrm{d}} I_{\mathrm{u}} \quad \text{and} \quad \frac{\mathrm{d}R_{\mathrm{d}}}{\mathrm{d}t} = \gamma_{\mathrm{d}} I_{\mathrm{d}}. \tag{4}$$

Some undetected cases after death are transferred to the hospital to be sure that the cause of death is COVID-19 infection, to be counted with deaths due to the virus at a rate $\rho$. Others are buried without being sure of this at a rate $b_{\mathrm{u}}$. As for confirmed cases after death, they are buried at a rate $b_{\mathrm{d}}$.

Then, the instantaneous change rates on the number of deaths and burials are given by the following three equations

$$\frac{\mathrm{d}D_{\mathrm{u}}}{\mathrm{d}t} = \mu_{\mathrm{u}} I_{\mathrm{u}} - (b_{\mathrm{u}} + \rho)D_{\mathrm{u}}, \quad \frac{\mathrm{d}D_{\mathrm{d}}}{\mathrm{d}t} = \mu_{\mathrm{d}} I_{\mathrm{d}} + \rho D_{\mathrm{u}} - b_{\mathrm{d}} D_{\mathrm{d}} \quad \text{and} \quad \frac{\mathrm{d}B}{\mathrm{d}t} = b_{\mathrm{u}} D_{\mathrm{u}} + b_{\mathrm{d}} D_{\mathrm{d}}. \tag{5}$$

Figure 1 illustrates the move schedule for that system and the nonlinear ODES (1)–(5) formulates the suggested model in this article.

$$\begin{cases} \frac{\mathrm{d}S}{\mathrm{d}t} = -\frac{(\beta_{\mathrm{u}} I_{\mathrm{u}} + \beta_{\mathrm{d}} I_{\mathrm{d}} + q D_{\mathrm{u}})S}{N}, \\ \frac{\mathrm{d}E}{\mathrm{d}t} = \frac{(\beta_{\mathrm{u}} I_{\mathrm{u}} + \beta_{\mathrm{d}} I_{\mathrm{d}} + q D_{\mathrm{u}})S}{N} - \sigma E, \\ \frac{\mathrm{d}I_{\mathrm{u}}}{\mathrm{d}t} = \tau\sigma E - (\mu_{\mathrm{u}} + \delta + \gamma_{\mathrm{u}})I_{\mathrm{u}}, \\ \frac{\mathrm{d}I_{\mathrm{d}}}{\mathrm{d}t} = (1-\tau)\sigma E + \delta I_{\mathrm{u}} - (\mu_{\mathrm{d}} + \gamma_{\mathrm{d}})I_{\mathrm{d}}, \\ \frac{\mathrm{d}D_{\mathrm{u}}}{\mathrm{d}t} = \mu_{\mathrm{u}} I_{\mathrm{u}} - (b_{\mathrm{u}} + \rho)D_{\mathrm{u}}, \\ \frac{\mathrm{d}D_{\mathrm{d}}}{\mathrm{d}t} = \mu_{\mathrm{d}} I_{\mathrm{d}} + \rho D_{\mathrm{u}} - b_{\mathrm{d}} D_{\mathrm{d}}, \\ \frac{\mathrm{d}R_{\mathrm{u}}}{\mathrm{d}t} = \gamma_{\mathrm{d}} I_{\mathrm{u}}, \\ \frac{\mathrm{d}R_{\mathrm{d}}}{\mathrm{d}t} = \gamma_{\mathrm{d}} I_{\mathrm{d}}, \\ \frac{\mathrm{d}B}{\mathrm{d}t} = b_{\mathrm{u}} D_{\mathrm{u}} + b_{\mathrm{d}} D_{\mathrm{d}}. \end{cases} \tag{6}$$

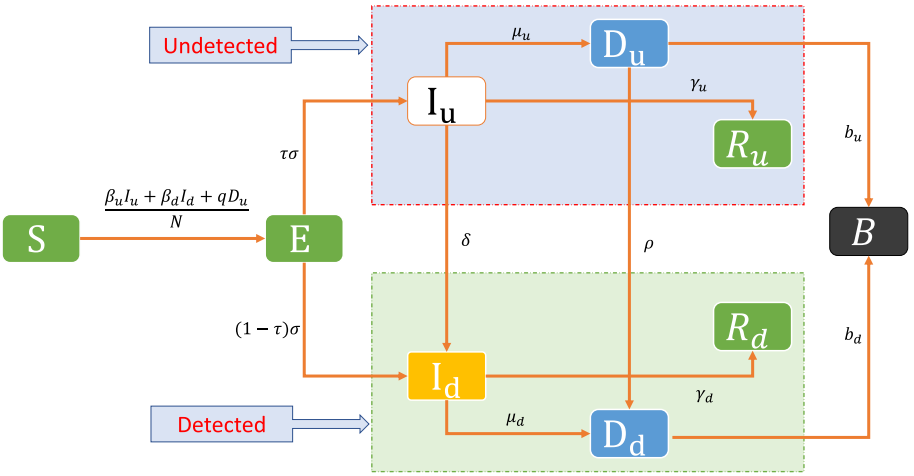


**Fig. 1** 2019-nCoV model schematic representation and specifications

**Table 1** Model parameters

| Parameters | Description |
|---|---|
| $\beta_u$ | Rate of transmission of infection from undetected cases |
| $\beta_d$ | Rate of transmission of infection from detected cases |
| $q$ | Rate of transmission of infection from death cases (at funerals) |
| $1/\sigma$ | Mean duration of the incubation period |
| $\tau$ | Proportion of exposed individuals transformed into infectious undetected after incubation |
| $\mu_d$ | Case fatality ratio of detected infected |
| $\mu_u$ | Case fatality ratio of undetected infected |
| $1/\gamma_d$ | Mean duration of the infection for detected |
| $1/\gamma_u$ | Mean duration of the infection for undetected |
| $\delta$ | Proportion of infected being detected |
| $\rho$ | Proportion of death being detected |
| $1/b_u$ | Mean time from death to burial for undetected |
| $1/b_d$ | Mean time from death to burial for detected |

All parameters used in the above model are listed with their description in Table 1. In our model, births and deaths (called vital dynamics) during the epidemic are not taken into account. In more detailed models, vital dynamics are included, see for example Brauer et al. (2012) and Ma (2009).

However, it is assumed in our paper that births and deaths exactly balance each other, so that the overall population size remains constant. The introduction of vital dynamics considerably modifies the dynamic behavior of the model. The constant population size assumption can be waived as in Korobeinikov and Wake (2002), see also Perakis et al. (2022, section 5.1). It turns out that there is no difference between the behavior of the dynamical system whether the population size remains constant or not. We, therefore, limit ourselves to the case of constant population.

## 3 Well-posedness of the model and equilibria

In this section, we prove that model (6) is well-posed. This is done in three steps below. At the beginning, we have to normalize the system (6) by using the following assertions: $x_1 = \frac{S}{N}, x_2 = \frac{E}{N}, x_3 = \frac{I_u}{N}, x_4 = \frac{I_d}{N}, x_5 = \frac{D_u}{N}, x_6 = \frac{D_d}{N}, x_7 = \frac{R_u}{N}, x_8 = \frac{R_d}{N}$ and $x_9 = \frac{B}{N}$ where the total population $N$ is assumed constant.

Since the compartments recovered undetected ($R_u$), recovered detected ($R_d$) and the buried ($B$) does not appear in the Eq. (6), then we can neglect them. Then the system (6) converted to the following normalized system:

$$\begin{cases} \frac{dx_1(t)}{dt} = -(\beta_u x_3(t) + \beta_d x_4(t) + q x_5(t))x_1(t), \\ \frac{dx_2(t)}{dt} = (\beta_u x_3(t) + \beta_d x_4(t) + q x_5(t))x_1(t) - \sigma x_2(t), \\ \frac{dx_3(t)}{dt} = \tau\sigma x_2(t) - (\mu_u + \delta + \gamma_u)x_3(t), \\ \frac{dx_4(t)}{dt} = (1-\tau)\sigma x_2(t) + \delta x_3(t) - (\mu_d + \gamma_d)x_4(t), \\ \frac{dx_5(t)}{dt} = \mu_u x_3(t) - (b_u + \rho)x_5(t), \\ \frac{dx_6(t)}{dt} = \mu_d x_4(t) + \rho x_5(t) - b_d x_6(t). \end{cases} \tag{7}$$

### 3.1 Well-posedness

**Theorem 1** *Assume that model (7) has a global solution corresponding to non-negative initial conditions. Then, the solution is non-negative at all time.*

***Proof*** Suppose that $x(t) = (x_1(t), \ldots, x_6(t))^T$ is any arbitrary global solution of the model (7) with the non-negative initial condition $x(0) = (x_1(0), \ldots, x_6(0))^T$. Now, suppose that $K(t) = (\beta_u x_3(t) + \beta_d x_4(t) + q x_5(t))$, then the first equation of the system can be written as follows

$$\frac{dx_1(t)}{dt} = -K(t)x_1(t), \tag{8}$$

which is a separable differential equation and its solution is of the form

$$x_1(t) = x_1(0)\exp\left(-\int_0^t K(y)dy\right), \tag{9}$$

since $x_1(0) \geq 0$, then the solution $x_1(t)$ in the Eq. (9) is non-negative, for any $t \in [0, \infty)$. To establish the non-negativity of other components of the solution $x(t)$, we pick up the following subsystem

$$\begin{cases} \frac{dx_2(t)}{dt} = (\beta_u x_3(t) + \beta_d x_4(t) + q x_5(t))x_1(t) - \sigma x_2(t), \\ \frac{dx_3(t)}{dt} = \tau\sigma x_2(t) - (\mu_u + \delta + \gamma_u)x_3(t), \\ \frac{dx_4(t)}{dt} = (1-\tau)\sigma x_2(t) + \delta x_3(t) - (\mu_d + \gamma_d)x_4(t), \\ \frac{dx_5(t)}{dt} = \mu_u x_3(t) - (b_u + \rho)x_5(t), \\ \frac{dx_6(t)}{dt} = \mu_d x_4(t) + \rho x_5(t) - b_d x_6(t). \end{cases} \tag{10}$$

Now, suppose that $Y(t) = (x_2(t), x_3(t), \ldots, x_6(t))^{\mathrm{T}}$ and $\mathcal{A}(t) =$
$$\begin{pmatrix} -\sigma & \beta_{\mathrm{u}}x_1(t) & \beta_{\mathrm{d}}x_1(t) & qx_1(t) & 0 \\ \tau\sigma & -(\mu_{\mathrm{u}}+\delta+\gamma_{\mathrm{u}}) & 0 & 0 & 0 \\ (1-\tau)\sigma & \delta & -(\mu_{\mathrm{d}}+\gamma_{\mathrm{d}}) & 0 & 0 \\ 0 & \mu_{\mathrm{u}} & 0 & -(b_{\mathrm{u}}+\rho) & 0 \\ 0 & 0 & \mu_{\mathrm{d}} & \rho & -b_{\mathrm{d}} \end{pmatrix}.$$
Then, the subsystem (10) has the following matrix representation

$$\dot{Y}(t) = \mathcal{A}Y(t). \tag{11}$$

We have to deal with the properties of the matrix $\mathcal{A}$. It is obvious that, the entries of the matrix has the property $a_{ij} \geq 0$, for all $i \neq j$, then the matrix $\mathcal{A}$ is Metzler matrix, which consequently leads that the matrix is monotone. Hence, the components of the solution $Y(t)$ is non-negative (Hal 1995). □

In the next theorem, we establish that the components of the solution of the model (7) are bounded.

**Theorem 2** *Suppose that $x(t) = (x_1(t), \ldots, x_6(t))^{\mathrm{T}}$ is any arbitrary global solution of the model (7) with the non-negative initial condition $x(0) = (x_1(0), \ldots, x_6(0))^{\mathrm{T}}$, where $x_i(0)$ is bounded for $i = 1:6$. Then $x_i(t)$ is bounded for $i = 1:6$ at any time.*

***Proof*** Let $K(t) = (\beta_{\mathrm{u}}x_3(t) + \beta_{\mathrm{d}}x_4(t) + qx_5(t))$. Then, the first equation of the model is reduced to the following separable differential equation

$$\frac{\mathrm{d}x_1(t)}{\mathrm{d}t} = -K(t)x_1(t). \tag{12}$$

It is easy to show $x_1(t) = x_1(0)\exp\left(-\int_0^t K(y)\mathrm{d}y\right)$ is the solution of (12). Since $0 \leq \exp\left(-\int_0^t K(y)\mathrm{d}y\right) \leq 1$ and $x_1(0)$ is bounded, then we conclude that $x_1(t)$ is bounded at any time $t$. From the second equation of the model (7) and using the boundedness property of $x_1(t)$, we obtain the following first-order linear ordinary differential equation

$$\begin{aligned} \frac{\mathrm{d}x_2(t)}{\mathrm{d}t} &= (\beta_{\mathrm{u}}x_3(t) + \beta_{\mathrm{d}}x_4(t) + qx_5(t))x_1(t) - \sigma x_2(t) \\ &\leq K(t)x_1(0)\exp\left(-\int_0^t K(t)\mathrm{d}t\right) - \sigma x_2(t) \\ &\leq -d\left(x_1(0)\exp\left(-\int_0^t K(t)\mathrm{d}t\right)\right) - \sigma x_2(t). \end{aligned} \tag{13}$$

The solution of the inequality (13) has the following form

$$\begin{aligned} x_2(t) &\leq x_2(0) + x_1(0)\exp(-\sigma t)\int_0^t \exp(\sigma s)\,K(s)\exp\left(-\int_0^s K(y)\mathrm{d}y\right)\mathrm{d}s \\ &\leq x_2(0) + x_1(0)\exp(-\sigma t)\left[-\exp(\sigma t)\exp\left(-\int_0^t K(y)\mathrm{d}y\right)\right. \\ &\quad \left. +\sigma\int_0^t \exp(\sigma s)\exp\left(-\int_0^s K(y)\mathrm{d}y\right)\mathrm{d}s\right] \\ &\leq x_2(0) + x_1(0)\exp(-\sigma t)\left[\exp(\sigma t) - 1\right] \\ &\leq x_2(0) + x_1(0) := \eta_2. \end{aligned} \tag{14}$$

Since $x_2(0)$ and $x_1(0)$ are bounded, then $x_2(t)$ is bounded at any time $t$. By using the boundedness of $x_2(t)$ in the remaining equations of (7), we obtain

$$x_3(t) \leq \frac{\tau\sigma(x_2(0)+x_1(0))}{\mu_u+\delta+\tau\sigma} := \eta_3, \tag{15}$$

$$x_4(t) \leq \frac{((1-\tau)\sigma(\mu_u+\delta+\tau\sigma)+\delta\tau\sigma)(x_2(0)+x_1(0))}{(\mu_u+\delta+\tau\sigma)(\mu_d+\gamma_d)} := \eta_4, \tag{16}$$

$$x_5(t) \leq \frac{\mu_u\tau\sigma(x_2(0)+x_1(0))}{(\tau\sigma+\rho)(\mu_u+\delta+\tau\sigma)} := \eta_5, \tag{17}$$

$$x_6(t) \leq \left[\frac{(1-\tau)\sigma\mu_d}{b_d} + \frac{\delta\tau\sigma\mu_d}{b_d(\mu_u+\delta\tau\sigma(\mu_d+\gamma_d))} + \frac{\rho\mu_u\tau\sigma}{(\tau\sigma+\rho)(\mu_u+\delta+\tau\sigma)b_d}\right] (x_2(0)+x_1(0)) := \eta_6. \tag{18}$$

Hence, $x_1, x_2, \ldots, x_6$ are bounded at any time. □

Because the initial point is non-negative. It is important to mention that the model (7) has the following positive invariant set

$$\mathcal{F} = \{(x_1, x_2, \ldots, x_6) \in \mathbb{R}^9 : 0 \leq x_1(t) \leq x_1(0), 0 \leq x_2(t) \leq \eta_2, 0 \leq x_3(t) \leq \eta_3, 0 \leq x_4(t) \leq \eta_4, 0 \leq x_5(t) \leq \eta_5, 0 \leq x_6(t) \leq \eta_6\}. \tag{19}$$

## 4 Basic reproduction number and equilibria

In this section, we establish the basic reproduction number and existence of equilibrium point of the model (7). To the beginning, we establish the steady-state equilibrium point of the model (7). Suppose that $(x_1^*, x_2^*, \ldots, x_6^*)$ is an equilibrium point of the model, then from the seventh and eighth equation of (7) we obtain the following

$$\gamma_d x_3^* = 0 \quad \text{and} \quad \gamma_d x_4^* = 0, \tag{20}$$

which they return that $x_3^* = x_4^* = 0$. Using these values in the fifth equation of (7), we obtain that $x_5^* = 0$ and from the sixth equation of (7), we have $x_5^* = 0$. Again using these values in other equations of (7), we obtain that $x_2^* = x_6^* = 0$. Hence, the equilibrium point of the model has the form $e = (x_1^*, 0, 0, 0, 0, 0)$, where $x_1^* \in \mathbb{R}^+$. We turn to calculate the basic reproduction number applying the next generation technique for the following subsystem

$$\begin{cases} \frac{dx_2(t)}{dt} = (\beta_u x_3(t) + \beta_d x_4(t) + q x_5(t))x_1(t) - \sigma x_2(t), \\ \frac{dx_3(t)}{dt} = \tau\sigma x_2(t) - (\mu_u + \delta + \gamma_u)x_3(t), \\ \frac{dx_4(t)}{dt} = (1-\tau)\sigma x_2(t) + \delta x_3(t) - (\mu_d + \gamma_d)x_4(t), \\ \frac{dx_5(t)}{dt} = \mu_u x_3(t) - (b_u + \rho)x_5(t), \\ \frac{dx_6(t)}{dt} = \mu_d x_4(t) + \rho x_5(t) - b_d x_6(t), \end{cases} \tag{21}$$

where the class of infection is $(x_2(t), x_3(t), x_4(t), x_5(t), x_6(t))$ and the ratio of infection class between the infection species is defined as follows

$$A(x_2(t), x_3(t), x_4(t), x_5(t), x_6(t)) = \begin{bmatrix} (\beta_u x_3(t) + \beta_d x_4(t) + q x_5(t))x_1(t) \\ 0 \\ 0 \\ 0 \\ 0 \end{bmatrix}. \tag{22}$$

The pace of all other viral class transfers is marked by

$$B\left(x_2(t), x_3(t), x_4(t), x_5(t), x_6(t)\right) = \begin{bmatrix} -\sigma x_2(t) \\ \tau\sigma x_2(t) - (\mu_u + \delta + \gamma_u)x_3(t) \\ (1-\tau)\sigma x_2(t) + \delta x_3(t) - (\mu_d + \gamma_d)x_4(t) \\ \mu_u x_3(t) - (b_u + \rho)x_5(t) \\ \mu_d x_4(t) + \rho x_5(t) - b_d x_6(t) \end{bmatrix}. \quad (23)$$

We have to compute the Jacobian matrix of $A$ and $B$ at the equilibrium point $e_1 = (0, 0, 0, 0, 0)$ for any arbitrary positive number $x_1^*$, then

$$\mathcal{A}(0,0,0,0,0) = \begin{bmatrix} 0 & \beta_u x_1^* & \beta_d x_1^* & q x_1^* & 0 \\ 0 & 0 & 0 & 0 & 0 \\ 0 & 0 & 0 & 0 & 0 \\ 0 & 0 & 0 & 0 & 0 \\ 0 & 0 & 0 & 0 & 0 \end{bmatrix} \quad (24)$$

and

$$\mathcal{B}(0,0,0,0,0) = \begin{bmatrix} -\sigma & 0 & 0 & 0 & 0 \\ \tau\sigma & -(\mu_u + \delta + \gamma_u) & 0 & 0 & 0 \\ (1-\tau)\sigma & \delta & -(\mu_d + \gamma_d) & 0 & 0 \\ 0 & \mu_u & 0 & -(b_u + \rho) & 0 \\ 0 & 0 & \mu_d & \rho & -b_d \end{bmatrix}. \quad (25)$$

Then, we have

$$\mathcal{A}\mathcal{B}^{-1}(0,0,0,0,0) = \begin{bmatrix} a_1 & a_2 & a_3 & a_4 & 0 \\ 0 & 0 & 0 & 0 & 0 \\ 0 & 0 & 0 & 0 & 0 \\ 0 & 0 & 0 & 0 & 0 \\ 0 & 0 & 0 & 0 & 0 \end{bmatrix}, \quad (26)$$

where

$$a_1 = \frac{-\beta_d x_1^*(\delta + (\gamma_u + \mu_u)(1-\tau))}{(\delta\gamma_d + \gamma_d\gamma_u + \delta\mu_d + \gamma_d\mu_u + \gamma_u\mu_d + \mu_d\mu_u)} - \frac{\mu_u q\tau}{b_u\delta + b_u\gamma_u + b_u\mu_u + \delta\rho + \gamma_u\rho + \mu_u\rho} - \frac{\beta_u\tau x_1^*}{\delta + \gamma_u + \mu_u}, \quad (27)$$

$$a_2 = \frac{-\mu_u q}{b_u\delta + b_u\gamma_u + b_u\mu_u + \delta\rho + \gamma_u\rho + \mu_u\rho} - \frac{\beta_u x_1^*}{\delta + \gamma_u + \mu_u} - \frac{\beta_d\delta x_1^*}{\delta\gamma_d + \gamma_d\gamma_u + \delta\mu_d + \gamma_d\mu_u + \gamma_u\mu_d + \mu_d\mu_u}, \quad (28)$$

$$a_3 = \frac{-\beta_d x_1^*}{\gamma_d + \mu_d} \quad \text{and} \quad a_4 = \frac{-q}{b_u + \rho}. \quad (29)$$

It is not difficult to show that $|a_1|$ is the spectral radius of the matrix $\mathcal{A}\mathcal{B}^{-1}(0,0,0,0,0)$. Then from the matrix and the next generation technique for the infection species we conclude that

$$\mathfrak{R}_D = \frac{\beta_{\mathrm{d}} x_1^*(\delta + (\gamma_{\mathrm{u}} + \mu_{\mathrm{u}})(1-\tau))}{(\delta\gamma_{\mathrm{d}} + \gamma_{\mathrm{d}}\gamma_{\mathrm{u}} + \delta\mu_{\mathrm{d}} + \gamma_{\mathrm{d}}\mu_{\mathrm{u}} + \gamma_{\mathrm{u}}\mu_{\mathrm{d}} + \mu_{\mathrm{d}}\mu_{\mathrm{u}})} + \frac{\mu_{\mathrm{u}} q\tau}{b_{\mathrm{u}}\delta + b_{\mathrm{u}}\gamma_{\mathrm{u}} + b_{\mathrm{u}}\mu_{\mathrm{u}} + \delta\rho + \gamma_{\mathrm{u}}\rho + \mu_{\mathrm{u}}\rho} + \frac{\beta_{\mathrm{u}}\tau x_1^*}{\delta + \gamma_{\mathrm{u}} + \mu_{\mathrm{u}}}, \tag{30}$$

$$= \mathfrak{R}_0 + \frac{\mu_{\mathrm{u}} q\tau}{b_{\mathrm{u}}\delta + b_{\mathrm{u}}\gamma_{\mathrm{u}} + b_{\mathrm{u}}\mu_{\mathrm{u}} + \delta\rho + \gamma_{\mathrm{u}}\rho + \mu_{\mathrm{u}}\rho}, \tag{31}$$

where

$$\mathfrak{R}_0 = \frac{\beta_{\mathrm{d}} x_1^*(\delta + (\gamma_{\mathrm{u}} + \mu_{\mathrm{u}})(1-\tau))}{(\delta\gamma_{\mathrm{d}} + \gamma_{\mathrm{d}}\gamma_{\mathrm{u}} + \delta\mu_{\mathrm{d}} + \gamma_{\mathrm{d}}\mu_{\mathrm{u}} + \gamma_{\mathrm{u}}\mu_{\mathrm{d}} + \mu_{\mathrm{d}}\mu_{\mathrm{u}})} + \frac{\beta_{\mathrm{u}}\tau x_1^*}{\delta + \gamma_{\mathrm{u}} + \mu_{\mathrm{u}}} \tag{32}$$

is the basic production number of the model without undetected class ($\tau = 0$), which really means, any deceased corpses contaminated are disposed properly.

## 5 Local stability of the equilibria

This section is devoted to study the local stability of the system (7) around the equilibrium point $e$. Throughout this section, we suppose that there is only transmission rate in community, then $\beta_{\mathrm{d}} = q = 0$. The basic reproduction reduces to the following equation

$$\mathfrak{R}_D = \frac{\beta_{\mathrm{u}}\tau x_1^*}{\delta + \gamma_{\mathrm{u}} + \mu_{\mathrm{u}}}.$$

The Jacobian matrix of the system at the equilibrium point has the following representation

$$J_e = \begin{bmatrix} 0 & 0 & -\beta_{\mathrm{u}} x_1^* & 0 & 0 & 0 \\ 0 & -\sigma & \beta_{\mathrm{u}} x_1^* & 0 & 0 & 0 \\ 0 & \tau\sigma & -(\mu_{\mathrm{u}} + \delta + \gamma_{\mathrm{u}}) & 0 & 0 & 0 \\ 0 & (1-\tau)\sigma & \delta & -(\mu_{\mathrm{d}} + \gamma_{\mathrm{d}}) & 0 & 0 \\ 0 & 0 & \mu_{\mathrm{u}} & 0 & -(b_{\mathrm{u}} + \rho) & 0 \\ 0 & 0 & 0 & \mu_{\mathrm{d}} & \rho & -b_{\mathrm{d}} \end{bmatrix}. \tag{33}$$

It is easy to compute the characteristic equation of the Jacobian matrix as follows

$$\lambda(\lambda + b_{\mathrm{u}})(\lambda + (b_{\mathrm{u}} + \rho))(\lambda + (\mu_{\mathrm{d}} + \gamma_{\mathrm{d}}))(\lambda^2 + (\sigma + \mu_{\mathrm{u}} + \delta + \gamma_{\mathrm{u}})\lambda + (\sigma(\mu_{\mathrm{u}} + \delta + \gamma_{\mathrm{u}}) - \beta_{\mathrm{u}}\tau\sigma x_1^*) = 0. \tag{34}$$

From the last factor of the characteristic equation, we obtain that

$$\lambda = \frac{-b \pm \sqrt{\Delta_0}}{2}, \tag{35}$$

where

$$\Delta_0 = b^2 - 4\beta_{\mathrm{u}}\tau\sigma x_1^*\left(\frac{1}{\mathfrak{R}_D} - 1\right) \quad \text{and} \quad b = \sigma + \frac{\beta_{\mathrm{u}}\tau x_1^*}{\mathfrak{R}_D}.$$

If $\mathfrak{R}_D < 1$, then $\Delta_0 < 0$. At this point, the real parts of every eigenvalues of the system at the equilibrium point $e$ are negative. Otherwise, at least the real part of one of the eigenvalues of the system is positive. According to this estimation we have the following result:

**Theorem 3** *In the absence of transmission rates of hospital and funerals by touching the dead body. The system (6) is locally stable around the equilibrium point e, where the reduced*

*basic reproduction number $\mathfrak{R}_D$ is less than one. On the other hand, if $\mathfrak{R}_D > 1$, then the system (6) is locally unstable around the equilibrium point e.*

## 6 Global stability of the equilibria

In this part, we investigate the global stability of the model (7) around the equilibrium point $e$. Suppose that $\beta_u$, $\beta_d$ and $q$ are arbitrary positive real numbers.

**Theorem 4** *The model (7) is globally stable around the equilibrium point e for any positive values of parameters, whenever the production number $\mathfrak{R}_D$ is less than one.*

***Proof*** Suppose that $X(t) = (x_1(t), x_2(t), \ldots, x_6(t)) \in \mathcal{F}$, then we define the Lyapunov function $\mathcal{V}(t) : \mathcal{F} \to \mathbb{R}^+$ by

$$\mathcal{V}(t) = x_1(t) - x_1^* - \ln\left(\frac{x_1(t)}{x_1^*}\right) + x_2(t) + \alpha_1 x_3(t) + \alpha_2 x_4(t) + \alpha_3 x_5(t) + \alpha_4 x_6(t). \quad (36)$$

The first derivative of $\mathcal{V}(t)$ is satisfying the following inequality, when we are using the Eq. (7)

$$\begin{aligned}\frac{\mathrm{d}\mathcal{V}(t)}{\mathrm{d}t} &= \frac{\mathrm{d}x_1(t)}{\mathrm{d}t}\frac{1}{x_1(t)}(x_1(t) - x_1^*) + \frac{\mathrm{d}x_2(t)}{\mathrm{d}t} + \alpha_1\frac{\mathrm{d}x_3(t)}{\mathrm{d}t} \\ &\quad + \alpha_2\frac{\mathrm{d}x_4(t)}{\mathrm{d}t} + \alpha_3\frac{\mathrm{d}x_5(t)}{\mathrm{d}t} + \alpha_4\frac{\mathrm{d}x_6(t)}{\mathrm{d}t} \\ &= [-1 + \alpha_1\tau + \alpha_2(1-\tau)]\sigma x_2(t) + [\beta_u x_1^* - \alpha_1(\mu_u + \delta + \gamma_u) + \alpha_2\delta + \alpha_3\mu_u]x_3(t) \\ &\quad + [\beta_d x_1^* - \alpha_2(\mu_d + \gamma_d) + \alpha_4\mu_d]x_4(t) + [q x_1^* - \alpha_3(b_u + \rho) + \alpha_4\rho]x_5(t) \\ &\quad + [-\alpha_4 b_d]x_6(t), \end{aligned} \quad (37)$$

where $\alpha_i, i = 1:4$ are real numbers satisfying the following system

$$\begin{cases} \beta_u x_1^* - \alpha_1(\mu_u + \delta + \gamma_u) + \alpha_2\delta + \alpha_3\mu_u = 0 \\ \beta_d x_1^* - \alpha_2(\mu_d + \gamma_d) + \alpha_4\mu_d = 0 \\ q x_1^* - \alpha_3(b_u + \rho) + \alpha_4\rho = 0 \\ -\alpha_4 b_d = 0. \end{cases} \quad (38)$$

By solving the system (38) for $\alpha_i, i = 1:4$ we obtain

$$\alpha_1 = \frac{\beta_u x_1^*}{(\mu_u + \delta + \gamma_u)} + \frac{\beta_d x_1^* \delta}{(\mu_d + \gamma_d)(\mu_u + \delta + \gamma_u)} + \frac{q x_1^* \mu_u}{(b_u + \rho)(\mu_u + \delta + \gamma_u)} \quad (39)$$

$$\alpha_2 = \frac{\beta_d x_1^*}{(\mu_d + \gamma_d)}, \quad \alpha_3 = \frac{q x_1^*}{(b_u + \rho)}, \quad \alpha_4 = 0. \quad (40)$$

Substituting the values of $\alpha_i$ in the Eq. (41), we obtain the following

$$\begin{aligned}\frac{\mathrm{d}\mathcal{V}(t)}{\mathrm{d}t} &= \left[-\sigma + \left[\frac{\beta_u x_1^*}{(\mu_u + \delta + \gamma_u)} + \frac{\beta_d x_1^* \delta}{(\mu_d + \gamma_d)(\mu_u + \delta + \gamma_u)} + \frac{q x_1^* \mu_u}{(b_u + \rho)(\mu_u + \delta + \gamma_u)}\right]\tau\sigma \right. \\ &\quad \left. + \left[\frac{\beta_d x_1^*}{(\mu_d + \gamma_d)}\right](1-\tau)\sigma\right] x_2(t) \\ &= \sigma[\mathcal{R}_D - 1] \le 0. \end{aligned} \quad (41)$$

Hence, the requirement of the theorem is obtained □

On the other hand, we have the following result for the case $\mathfrak{R}_D > 1$. we can prove that, the model (7) is unstable around the equilibrium point $e$ for any positive values of parameters, whenever the production number $\mathfrak{R}_D$ is greater than one.

Note that model (7) has no endemic equilibrium, so the only constant solution exists is free disease equilibrium, but if we do not neglect the effect of vital dynamics, the model must have endemic equilibrium, some works that deal with COVID-19 and other infectious diseases without endemic equilibrium are found in de Barros et al. (2021), Watve et al. (2021), Ram and Schaposnik (2021), Da Silva (2021) and Gao et al. (2016).

## 7 Simulations and model mathematical validation

### 7.1 Data collection

From the main publicly available sources, we acquired authentic COVID-19 data for Morocco: A maximum number of case(s) in Morocco are gathered by the World Health Organization (WHO) and Worldometer (2020), current diagnoses, reported infections everyday, new innovative deaths, death and bury. The total population of Morocco in 2018 was 36,029,093, see Worldometers (2020b).

### 7.2 Estimation of unknown parameters and undetected cases in Morocco

Throughout contrast to estimating the number of non-detected patients, recuperated instances and fatalities, this part will provide the least squares approach for estimating values of the parameters and adapting the system to actual data. We make a simple modification on model (6) by dividing the compartment of deceased and buried cases ($B$) into two groups, undetected and buried death ($B_{\mathrm{u}}$) and detected and buried death ($B_{\mathrm{d}}$). Then the instantaneous change rates on the number of burials undetected and burials detected are, respectively, given by the following two equations

$$\frac{\mathrm{d}B_{\mathrm{u}}}{\mathrm{d}t} = b_{\mathrm{u}} D_{\mathrm{u}}, \quad \frac{\mathrm{d}B_{\mathrm{d}}}{\mathrm{d}t} = b_{\mathrm{d}} D_{\mathrm{d}}. \tag{42}$$

We consider the model solution

$$Z(t) = (S(t), E(t), I_{\mathrm{u}}(t), I_{\mathrm{d}}(t), D_{\mathrm{u}}(t), D_{\mathrm{d}}(t), R_{\mathrm{u}}(t), R_{\mathrm{d}}(t), B_{\mathrm{u}}(t), B_{\mathrm{d}}(t)),$$

depending on the vector of parameters $\theta = (\beta_{\mathrm{u}}, \beta_{\mathrm{d}}, q, \sigma, \tau, \gamma_{\mathrm{u}}, \gamma_{\mathrm{d}}, \delta, \rho, \mu_{\mathrm{u}}, \mu_{\mathrm{d}}, b_{\mathrm{u}}, b_{\mathrm{d}})$, the initial conditions $Z(t_0) = Z_0$.

Initial values $I_{\mathrm{d}}(0)$, $R_{\mathrm{d}}(0)$, $D_{\mathrm{d}}(0)$ and $B_{\mathrm{d}}(0)$ are recognized to be found in COVID-19; however, the information are not accessible as $S(0)$, $E(0)$, $I_{\mathrm{u}}(0)$, $R_{\mathrm{u}}(0)$, $D_{\mathrm{u}}(0)$ and $B_{\mathrm{u}}(0)$. The unknown parameter must be in an interval of type $[m, M]$ with $m$ and $M$ are, respectively, the maximum and minimum values of this parameter according to its biological interpretation, in the following notes we give the justification for the choice of range or value of each parameter.

- **Transmission rates:** Any susceptible individual can be infected by another infectious individual, this is done by a transmission rate, in our model we have three transmission rates $\beta_{\mathrm{u}}$ $\beta_{\mathrm{d}}$ and $q$ these rates are measured in effective contacts per unit time. Each rate can be expressed as the product of the total contact rate and the risk of infection (or risk of transmission), so the transmission rate is chosen to be a positive value. In general,

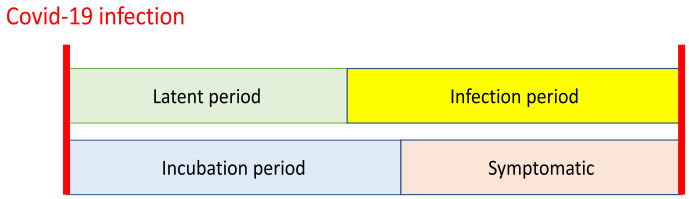


**Fig. 2** Key time periods of COVID-19 infection: latent period, incubation period, infection period and symptomatic period

the two rate $\beta_d$ and $\beta_u$ cannot be compared because the possibility of transmission of the virus has to do with the nature of the country and the nature of the movement, the imposition of quarantine or not, etc. Moreover, the presence of undetected cases which will be confirmed later with two rates $\delta$ (from $I_u$ to $I_d$) and $\rho$ (from $D_u$ to $D_d$). Moreover in Li et al. (2020) the authors consider $\beta_u$ is a reduction of $\beta_d$ then $\beta_d \geq \beta_u$.

- **Incubation rate** ($\sigma$): is the rate of latent individuals becoming infectious (average period of stay in state exposed compartment E), the reciprocal is the incubation period $1/\sigma$ (see Fig. 2), this value is varied from country to country, it must be estimated in an interval, depending on the work carried out for COVID-19. In this study, we estimate this value between 2 and 5 days, see Worldometers (2020a) for more discussion about Coronavirus incubation period.
- **Recovery rate:** is the rate of infected individuals becoming recovered from the disease (see Fig. 2), in our COVID-19 model, we have the recovery rate of detected individuals $\gamma_d$, and the recovery rate of undetected individuals $\gamma_u$, then the average duration of infection for infected and detected individuals ($1/\gamma_d$) is not necessarily the same as undetected individuals ($1/\gamma_u$). The average duration of infection for infected and undetected individuals is fixed in 14 days (Mahajan et al. 2021) and assume that the average duration of infection for detected individuals is estimated in the interval 10–18 days (confidence interval of 71.42%).
- **Burial rate:** the rate for a deceased individual (due to COVID-19) to be buried (reciprocal is the burial period), in Morocco and in all Islamist countries each dead person, must be buried within one or two days after death, so we will estimate the two parameters $1/b_u$ and $1/b_d$ between 0 and 2 days (see Table 2). In Morocco, confirmed cases of death due to COVID-19 are delayed in burial compared to natural undetected deaths (or natural deaths) (this mean that $1/b_u \leq 1/b_d$), among the reasons for the delay is after hospitals and the procedures accompanying the burial license or the recovery of medical expenses, see also Corona in Morocco (2022) and Burial rites in Morocco (2022).
- **Case fatality ratio of COVID-19:** is the proportion of individuals infected with COVID-19 who die, therefore, the values of $\mu_d$ and $\mu_u$ are very close to zero, so we can estimate its values in Morocco in a small interval [0–0.1] (see Table 2).

The other parameters $\tau$, $\delta$ and $\rho$ are proportions estimated between 0 and 1. For the unknown initial values, it is necessary to choose a maximum value of each compartment according to the onset time and the nature of the disease.

Since this model is applied for the first time to the real data of Morocco (for COVID-19), then the parameters must be estimated except the duration of infection for undetected infected $\gamma_u = 1/14$ which fixed at 14 according to Mahajan et al. (2021), the results can be improved if we add other data, but for our case, we used the possible data and published on the internet.

**Table 2** The comparison between the parameters estimated for the case of Morocco studied in the current paper using real data with the parameters obtained in the literature for the other countries: Germany (Mahajan et al. 2021), South Korea (Mahajan et al. 2021), USA (Mahajan et al. 2021), China (Ivorra et al. 2020), and India (Mahajan et al. 2020)

| Parameters | Morocco | | | | Germany (Mahajan et al. 2021) | South Korea (Mahajan et al. 2021) | USA (Mahajan et al. 2021) | China (Ivorra et al. 2020) | India (Mahajan et al. 2020) |
|---|---|---|---|---|---|---|---|---|---|
| | Range | Phase 1 | Phase 2 | Source | | | | | |
| $\beta_u$ | Positive | 0.10138 | 0.10138 | Fitted | [0.11, 0.35] | [0.11, 0.45] | [0.11, 0.35] | [0.1739, 0.2650] | [0.09, 0.35] |
| $\beta_d$ | Positive | 0.99 | 5.7436 | Fitted | 9E−3 | 5.9E−3 | 6E−3 | [0.0052, 0.0924] | 6E−3 |
| $q$ | Positive | 1 | 1 | Fitted | – | – | – | – | – |
| $\sigma$ | [1/5, 1/2] | 0.44773 | 0.2 | Fitted | [0.272, 1] | [0.272, 1] | [0.272, 1] | 0.1818 | – |
| $\tau$ | [0, 1] | 0.97816 | 0.92506 | Fitted | – | – | – | [0.35, 0.86] | – |
| $\mu_d$ | [0, 0.1] | 3.7E−4 | 3.7E−4 | Fitted | Variable | Variable | Variable | [0.005, 0.022] | 2E−03 |
| $\mu_u$ | [0, 0.1] | 4.2E−4 | 4.2E−4 | Fitted | – | – | – | [0.005, 0.022] | – |
| $\gamma_d$ | [1/18, 1/10] | 0.09859 | 0.06859 | Fitted | 0.065 | 0.034 | 0.017 | [0.0752, 0.1370] | 0.065 |
| $\gamma_u$ | – | 0.07 | 0.07 | Mahajan et al. (2021) | 0.07 | 0.07 | 0.07 | [0.0752, 0.1370] | 0.07 |
| $\delta$ | [0, 1] | 1.81E−07 | 1.81E−07 | Fitted | [1.67E−6, 1] | [2.05E−5, 1] | [0, 1] | – | [5.7E−3, 1] |
| $\rho$ | [0, 1] | 0.31683 | 0.40816 | Fitted | – | – | – | – | – |
| $1/b_u$ | [0, 2] | 0.2 days | 0.2 days | Fitted | – | – | – | – | – |
| $1/b_d$ | [0, 2] | 0.378 days | 0.378 days | Fitted | – | – | – | – | – |
| $N$ | – | 3.60E6 | 3.60E6 | Worldometers (2020b) | 8.30E7 | 5.10E7 | 3.31E8 | 1.4E9 | 1.38E9 |

In general, the parameters are time-dependent variables (see for example Liu and Stechlinski 2012; Al-Salti et al. 2021), but due to the difficulties of determining their expression, the authors consider them constant and seek to estimate their average values, but when studying a long period this estimate will not be erased, to avoid this problem we divide the period and propose different phases (three phases are considered in Huo et al. 2021) and vary some parameters who has the greatest impact, in our paper, we consider two phases and we vary the two transmission rates $\beta_u$ and $\beta_d$.

The vector of parameters to be estimated belongs to a set given by

$$\Pi = \{(\mathcal{P}, \mathbb{X}_0) \in \mathbb{R}^{12} \times \mathbb{R}^6 / \mathcal{L}_b \leq (\mathcal{P}, \mathbb{X}_0) \leq \mathcal{U}_b\}.$$

In which the lowest and highest vectors of both $\mathcal{L}_b$ and $\mathcal{U}_b$ are the parameters for the model (and the startup numbers). $\mathcal{P}$ is the vectors of all model parameters except $\gamma_u$ and $\mathbb{X}_0 = (S(0), E(0), I_u(0), R_u(0), D_u(0), B_u(0))$ vectors of the initial values to estimated.

The choice of lower and upper values $\mathcal{L}_b$ and $\mathcal{U}_b$ in general is not arbitrary, the ranges used for the parameters to be estimated are given in Table 3 and this choice already explained previously, for the ranges of the initial conditions $\mathbb{X}_0 = (S(0), E(0), I_u(0), R_u(0), D_u(0), B_u(0))$ the following remarks are given

- The choice of unknown initial values $\mathbb{X}_0$ is sensitive to the model solutions, i.e., the total number of undetected infected can be can be far from the real number of cases if the initial number chosen is too far from the one in reality.
- It is preferable to choose the initial state is in the first days of the appearance of COVID-19, in this case, a reasonable range can be chosen easily (the number of infected cases is smaller).
- A range of $R_0$ in the Literature can be used to determine the range of the initial conditions (exposed, infected undetected, etc.).

In our case, we choose the reasonable ranges to obtain the estimated values of the initial values, these ranges are given in the Table 3.

Let $\text{Idata}_k$, $\text{Ddata}_k$, $\text{Rdata}_k$, and $\text{Bdata}_k$ values of observed data of infected active cases, daily death, recovered, and burial, respectively, at given times $t_k, k = 1, \ldots n$.

When we fix $\Pi$ we compute the numerical solutions of the model using of Runge–Kutta numerical method which is predefined in MATLAB by a function named ODE45, denote

**Table 3** Estimated initial values

| Initial conditions | Range | Value | Source |
|---|---|---|---|
| $N$ | – | 36,029,093 | Worldometers (2020b) |
| $S(0)$ | – | 36,027,528 | Calculated |
| $E(0)$ | 6–1000 | 829 | Estimated |
| $I_u(0)$ | 6–800 | 700 | Estimated |
| $I_d(0)$ | – | 6 | Worldometer (2020) |
| $R_d(0)$ | – | 1 | Worldometer (2020) |
| $R_u(0)$ | 1–80 | 19 | Estimated |
| $D_d(0)$ | – | 0 | Worldometer (2020) |
| $D_u(0)$ | 1–8 | 7 | Estimated |
| $B_u(0)$ | 1–8 | 2 | Estimated |
| $B_d(0)$ | – | 1 | Worldometer (2020) |

these output vectors by $\{I(t_k, \Pi)\}$ for infected, by $\{D(t_k, \Pi)\}$ for daily deaths, by $\{R(t_k, \Pi)\}$ for recovered by $\{B(t_k, \Pi)\}$ for buried. We consider the four objective functions $\mathcal{F}_1$, $\mathcal{F}_2$, $\mathcal{F}_3$, and $\mathcal{F}_4$ defined by

$$\mathcal{F}_1(\Pi) = \frac{1}{n}\sum_{k=1}^{n} \left(I(t_k, \Pi) - \text{Idata}_k\right)^2,$$

$$\mathcal{F}_2(\Pi) = \frac{1}{n}\sum_{k=1}^{n} \left(D(t_k, \Pi) - \text{Ddata}_k\right)^2,$$

$$\mathcal{F}_3(\Pi) = \frac{1}{n}\sum_{k=1}^{n} \left(R(t_k, \Pi) - \text{Rdata}_k\right)^2,$$

$$\mathcal{F}_4(\Pi) = \frac{1}{n}\sum_{k=1}^{n} \left(B(t_k, \Pi) - \text{Bdata}_k\right)^2.$$

Aimed to find the set of parameters that minimizes the differences between the observed and the predicted data, we formulate the following multi-objective Least Squares problem:

$$\begin{cases} \min\left(\mathcal{F}_1(\Pi), \mathcal{F}_2(\Pi), \mathcal{F}_3(\Pi), \mathcal{F}_4(\Pi)\right) \\ \text{subject to} \\ \mathcal{L}_b \le \Pi \le \mathcal{U}_b, \\ I(t_k, \Pi),\ D(t_k, \Pi),\ R(t_k, \Pi) \text{ and } B(t_k, \Pi) \text{ are the computed numerical} \\ \text{solution of the model (6) for given parameters vector } \Pi. \end{cases} \tag{43}$$

One of the most used methods to solve the multi-objective problem (43) is to replace the multi-objective function by the objective function defined by the sum of the objectives $\mathcal{F}_1$, $\mathcal{F}_2$, $\mathcal{F}_3$ and $\mathcal{F}_4$:

$$\mathbb{F}(\Pi) = \mathcal{F}_1(\Pi) + \mathcal{F}_2(\Pi) + \mathcal{F}_3(\Pi) + \mathcal{F}_4(\Pi). \tag{44}$$

This method was used by Mahajan et al. (2020, 2021) to predict the total number of infected and active cases of COVID-19 in India and USA respectively. But in our case we also want to predict the number of Coronavirus (COVID-19) recoveries, and deaths in Morocco. We want to estimate the number of cases detected infected, recovered, died. When we use the standard least squares method which seeks to minimize the function $F$ given in (44) we can lose some information on the data of deaths, because the real data of recovered are greater in comparison with the data of deaths, therefore to extract a maximum of Information from small data sets (e.g., number of deaths), We are using the weighted sum technique. This strategy is much more efficient if the data sets are of various quality, see Yang (2014), Gunantara (2018) and Deb (2014).

The new objective function can be written as:

$$\mathbb{F}_w(\Pi) = \mathcal{F}_{w1}(\Pi) + \mathcal{F}_{w2}(\Pi) + \mathcal{F}_{w3}(\Pi) + \mathcal{F}_{w4}(\Pi), \tag{45}$$

such as

$$\mathcal{F}_{w1}(\Pi) = \frac{1}{n}\sum_{k=1}^{n} w_k^1 \left(I(t_k, \Pi) - \text{Idata}_k\right)^2,$$

$$\mathcal{F}_{w2}(\Pi) = \frac{1}{n}\sum_{k=1}^{n} w_k^2 \left(D(t_k, \Pi) - \text{Ddata}_k\right)^2,$$

$$\mathcal{F}_{w3}(\Pi) = \frac{1}{n}\sum_{k=1}^{n} w_k^3 \left(R(t_k, \Pi) - \text{Rdata}_k\right)^2,$$

$$\mathcal{F}_{w4}(\Pi) = \frac{1}{n}\sum_{k=1}^{n} w_k^4 \left(B(t_k, \Pi) - \text{Bdata}_k\right)^2,$$

and $w_k^1$, $w_k^2$, $w_k^3$, and $w_k^4$, $k = 1, 2, \ldots,$ are constant weights, it is the usual practice to choose weights such that their sum is one, or $\frac{1}{n}\sum_{i=1}^{4} w_k^i = 1$, see Yang (2014), Gunantara (2018) and Deb (2014) for more details.

To estimate the model parameters, we use three-step approach.

1. The first step is solving the ordinary differential equation given in (6), using Runge–Kutta 4th order method.
2. We use the Nelder–Mead simplex algorithm as described in Lagarias et al. (1998) to solve our least square problem. In Matlab program, the function *fmincon* is used to find the optimal values of the parameters. The variables of this function are the following:
   - The objective function whose variables are the parameters to be estimated, it returns the value of the function $\mathbb{F}_w$ given by (45), inside this function the 4th order Runge–Kutta method which is predefined on Matlab by *ode45* is applied to solve the proposed COVID-19 model and then calculates the sum of squared residuals.
   - The initial values of the parameters and the initial conditions.
   - The lower and upper values of the parameters and the initial conditions to be estimated.
   - The precision provided because the solution obtained by this function is local so the function stops when the best precision is found.

   The output of this function are the optimal values of the parameters as well as the value of objective function $F_w$ obtained using these parameters.
3. Updating the parameters continues until no significant improvement in the objective function is observed.

The detail of the Nelder–Mead simplex algorithm used to estimate the model parameters is given in Algorithm 1.

In the absence of data from the buried in Morocco, and the actual death case of COVID-19 in Morocco are considered buried, so we only consider the three functions $\mathcal{F}_{w1}$, $\mathcal{F}_{w3}$, and $\mathcal{F}_{w4}$ and the three weights are chosen as follows

$$w_k^1 = 4/11,\ w_k^3 = 1/11,\ w_k^4 = 8/11, \quad k = 1, 2, \ldots, n$$

note that these constants are chosen so that the data must normalized.

If the parameters are estimated using the reported cases (infected detected $I_{\text{u}}$, recovered detected $R_{\text{d}}$, daily death detected $D_{\text{d}}$, total death detected and buried $B_{\text{d}}$) we use the fixed and estimated parameters with the initial conditions (estimated or fixed) and we solve our model, we find the system of model solutions, the compartments $I_{\text{u}}$, $R_{\text{u}}$ and $D_{\text{u}}$ must be compared with the real data to show the effectiveness of this fitting, and the compartments $I_{\text{u}}$, $R_{\text{u}}$ and $D_{\text{d}}$ represent the estimated undetected (unreported) cases, the sums between detected and undetected cases represent the sums between detected and undetected cases represent the true total number of COVID-19 cases.

Here, we are investigating the actual data of COVID-19 in Morocco from 13 March 2020 to 4 August 2021 provided by the World Health Organization (WHO).

**Algorithm 1** An algorithm to estimate model parameters Lagarias et al. (1998); Barati (2011); Fuh and Tsai (2019)

**Require:** Observed data of Infected **Idata**, Deaths **Ddata**, and Recovered **Rdata**.
The initial parameter set $\Pi = (\mathcal{P}, \mathbb{X}_0)$ that needs to be optimized.
The constant weights $w_k^1$, $w_k^2$, and $w_k^3$, $k = 1, 2, .., n$.
The constant weights $w_k^1$, $w_k^2$, and $w_k^3$, $k = 1, 2, .., n$.
Algorithm parameters $\vartheta_1$, $\vartheta_2$, $\vartheta_3$ and $\vartheta_4$.
**Ensure:** The optimal parameter set $(\mathcal{P}^*, \mathbb{X}_0^*)$.

1: Give an initial simplex comprising $m+1$ vertices $\Pi^0 = (\mathcal{P}^0, \mathbb{X}_0^0), \Pi^1 = (\mathcal{P}^1, \mathbb{X}_0^1), \ldots, \Pi^m = (\mathcal{P}^m, \mathbb{X}_0^m)$
2: Calculate function values $\mathbb{F}^0, \mathbb{F}^1, \ldots, \mathbb{F}^m$ corresponding to $\Pi^0, \Pi^1, \ldots, \Pi^m$.
3: **Order**: Order the $m+1$ vertices to meet $\mathbb{F}^0 \leq \mathbb{F}^1 \leq \ldots \leq \mathbb{F}^m$.
4: **Reflect**:Calculate the reflection point $\Pi_r$ by

$$\Pi_r = \bar{\Pi} + \vartheta_1 \left(\bar{\Pi} - \Pi^m\right), \quad (\vartheta_1 > 0),$$

where $\bar{\Pi} = (1/m) \sum_{i=0}^{m-1} \Pi^i$ = centroid of the $m$ best points. Also calculate $\mathbb{F}_r = \mathbb{F}_w(\Pi_r)$. If $\mathbb{F}_0 \leq \mathbb{F}_r < \mathbb{F}_{m-1}$, accept the reflected point $\Pi_r$ and terminate the iteration.
5: **Expand**: If $\mathbb{F}_r < \mathbb{F}_0$, compute the expansion point $\Pi_e$ by

$$\Pi_e = \bar{\Pi} + \vartheta_2 \left(\Pi_r - \bar{\Pi}\right), \quad (\vartheta_2 > 1 \quad \text{and} \quad \vartheta_2 > \vartheta_1).$$

Also calculate $\mathbb{F}_e = \mathbb{F}_w(\Pi_e)$. If $\mathbb{F}_e < \mathbb{F}_r$, accept $\mathbb{F}_e$, and terminate the iteration; otherwise (if $\mathbb{F}_e \geq \mathbb{F}_r$ ), accept $\Pi_r$ and terminate the iteration.
6: **Contract**: If $\Pi_r \geq \mathbb{F}_{m-1}$, execute a contraction between $\bar{\Pi}$ and the better of $\Pi_m$ and $\Pi_r$.
a. **Outside**. If $\mathbb{F}_{m-1} \leq \mathbb{F}_r < \mathbb{F}_m$, compute the outside contraction point $\Pi_c$ by

$$\Pi_c = \bar{\Pi} + \vartheta_3 \left(\Pi_r - \bar{\Pi}\right), \quad (0 < \vartheta_3 < 1).$$

Also calculate $\mathbb{F}_c = \mathbb{F}(\Pi_c)$. If $\mathbb{F}_c < \mathbb{F}_r$, accept $\Pi_c$ and terminate the iteration; otherwise, continue with step 7.
b. **Inside**: If $\mathbb{F}_r \geq \mathbb{F}_m$, compute the inside contraction point $\Pi_{cc}$ by

$$\Pi_{cc} = \bar{\Pi} - \vartheta_3 \left(\bar{\Pi} - \Pi_{n+1}\right).$$

Also calculate $\mathbb{F}_{cc} = \mathbb{F}_w(\Pi_{cc})$. If $\mathbb{F}_{cc} < \mathbb{F}_m$, accept $\Pi_{cc}$ and terminate the iteration; otherwise, continue with step 7.
7: **Shrink**: Compute the $m-1$ points by

$$\Sigma_i = \Pi_1 + \vartheta_4 (\Pi_0 - \Pi_0), \quad (0 < \vartheta_4 < 1).$$

Also calculate $\mathbb{F}(\Sigma_i), i = 1, \ldots, m$. The unordered vertices of the simplex at the next iteration are composed of $\Pi_0, \Sigma_1, \ldots, \Sigma_m$.
If the termination criteria are satisfied, end the iteration procedure; else go to Step 2.

The initial values of detected infected ($I_{\mathrm{d}}(0)$), detected deaths not buried ($D_{\mathrm{d}}(0)$), total deaths detected and buried ($B_{\mathrm{d}}(0)$) and recovered detected ($R_{\mathrm{d}}(0)$) are known by the real data but we do not know the initial values of other compartments in this case, it is necessary to estimate these. We consider March 13, 2020 to be the initial state and we predict the model for 510 days after, on this date, Morocco recorded 8 confirmed cases, including one recovered and one death (buried), until August 4, 2021, Morocco has confirmed 653,286 total cases, 582,692 recovered, 60,579 active case (infected) and 10,015 confirmed death cases.

First, the parameter intervals should be selected to restrict the search for the parameter values. Then, the intervals of each parameters are given in Table 2. This uncertainty is interpreted by the constraints of the inequalities in the optimization problem described in (43).

Figures 3, 4, 5 and 6 show the model fitted to actual data of COVID-19 in Morocco (infected detected deaths detected and recovered detected) from March 13, 2020 to August 04, 2021. We notice that our model gives a reasonable adjustment to the real data (Figs. 7, 8, 9, 10, 11, 12). The estimated parameters and initial values are presented in Tables 2 and 3.

To demonstrate the quality of the fit of the model, we present in the form of bar graphs in Fig. 13 the comparison between the real data and thus predicts the total number of detected and undetected cases of COVID-19 in Morocco. The detected and undetected cases per month from March 2020 until July 2021 in Morocco are given in Table 4, after these simulation results, we can conclude that until August 4, 2021:

- In Morocco, the overall incidences of COVID-19 infections, comprising 653,286 patients diagnosed is 24,663,240, compared with 24,009,954 undetected, i.e., a detection rate of 2.65%.

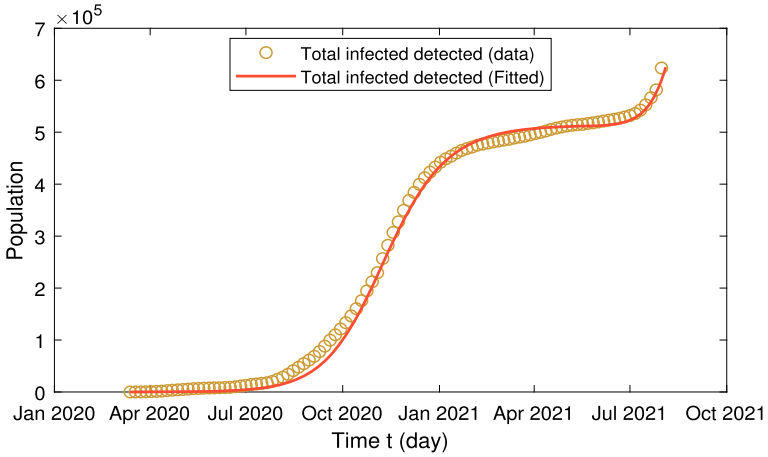


**Fig. 3** The predicted total detected cases ($I_d + R_d + B_d$) compared with the real data of them in Morocco from March 13, 2020 to August 04, 2021

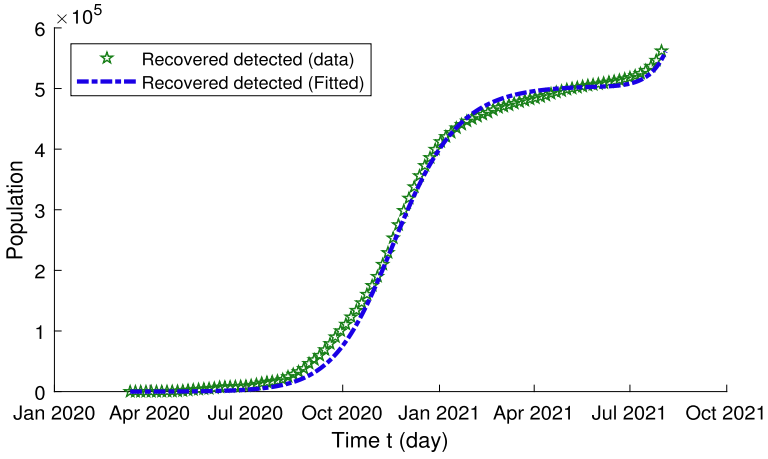


**Fig. 4** The predicted Recovered detected cases ($R_d$) compared with the actual number of them in Morocco from March 13, 2020 to August 04, 2021

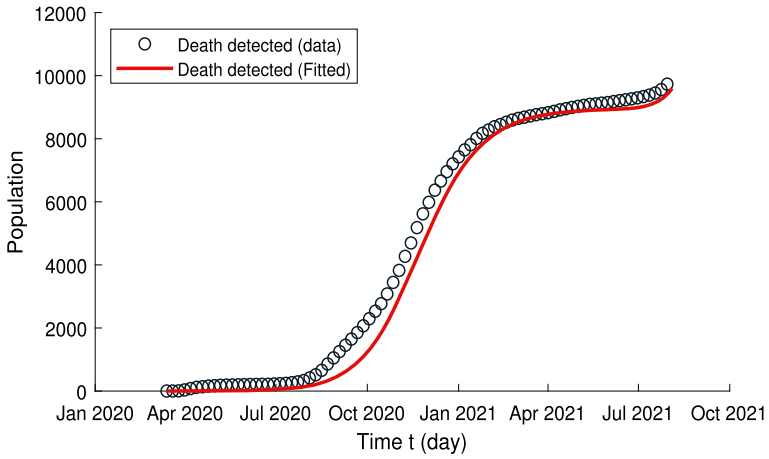


**Fig. 5** The predicted Deaths detected cases ($B_d$) compared with the total number of them in Morocco from March 13, 2020 to August 04, 2021

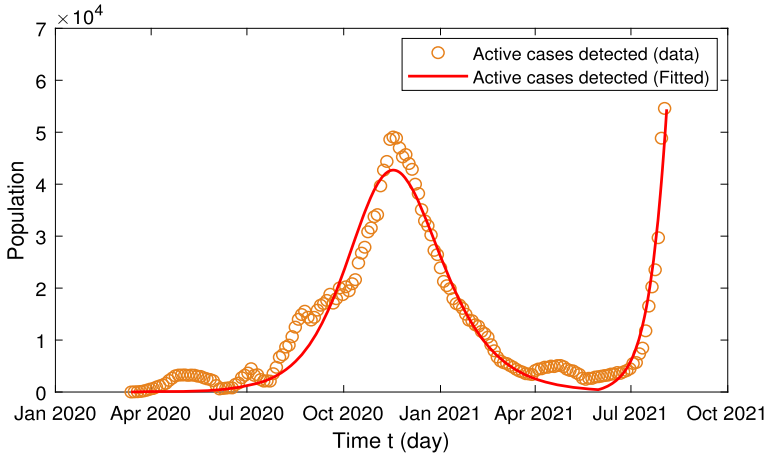


**Fig. 6** The predicted active cases detected ($I_d$) compared with the real data of them in Morocco from March 13, 2020 to August 04, 2021

- The total number of recovered cases of COVID-19 in Morocco is 23,818,616, including 582,692 confirmed cases, against 23,235,924 undetected, i.e. a detection rate of 2.45%.
- The total number of death cases of COVID-19 in Morocco is 126,248, including 10,015 confirmed cases, against 116,233 undetected, for a detection rate of 7.83%.

### 7.3 Forecasting and different scenarios

In this section, various scenarios have been treated graphically using the model described above, the number of cases varies according to the transmission rates and the detection rate (number of tests), i.e., increase or decrease in values. Several scenarios are fully represented graphically in Figs. 14, 15, 16, 17, 18, 19, 20, 21, 22, 23, 24, 25 and 26.

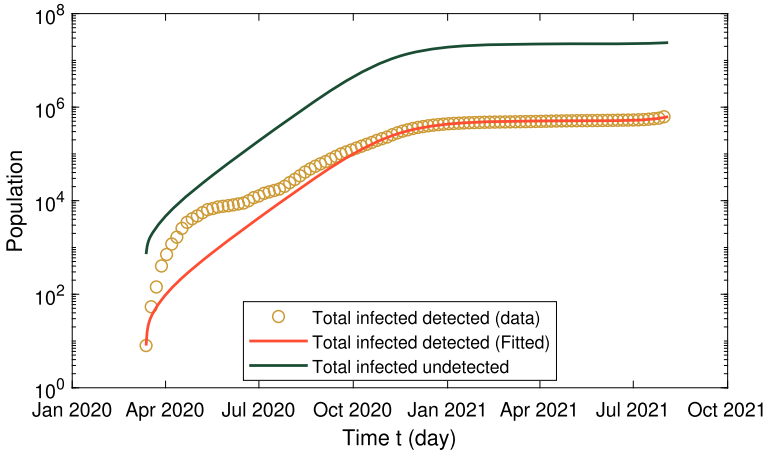


**Fig. 7** The predicted detected ($I_d + R_d + B_d$) and undetected ($I_u + R_u + B_u$) total cases compared with the total confirmed cases in Morocco from March 13, 2020 to August 04, 2021

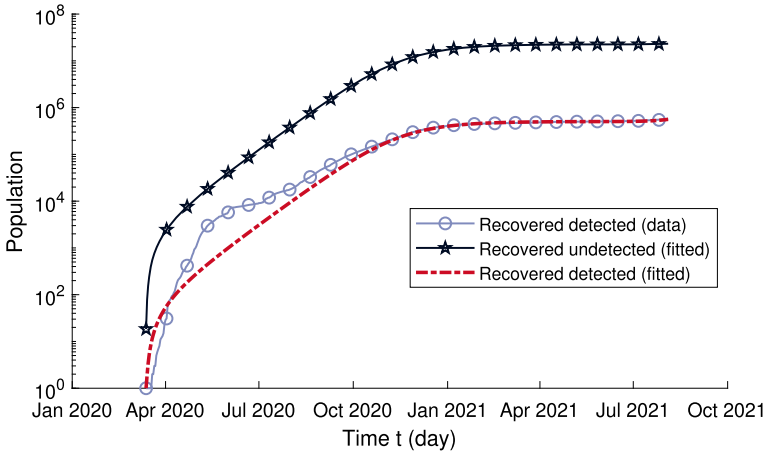


**Fig. 8** The predicted Recovered detected ($R_d$) and undetected cases ($R_u$) compared with the actual number of recovered in Morocco from March 13, 2020 to August 04, 2021

From Figs. 20, 21 and 22, it can be concluded that the rate of transmission of infection from deceased cases has a small effect on the increase and decrease in the number of cases, which is normal because the number of daily deaths are very low compared to active cases of COVID-19. The reduction of $\tau$ means the increase in detection rate, in Figs. 23, 25 and 26, we notice that if we reduce the value of $\tau$, then the number of infected cases increases, but on the other hand, the number of undetected cases reduces, see Fig. 24.

According to these results, the continuation of the current situation as it is, it is expected that the number of cases in December 2021 will reach about 139,6450 cases, including 18,982 deaths. In the following lines, we discuss several scenarios:

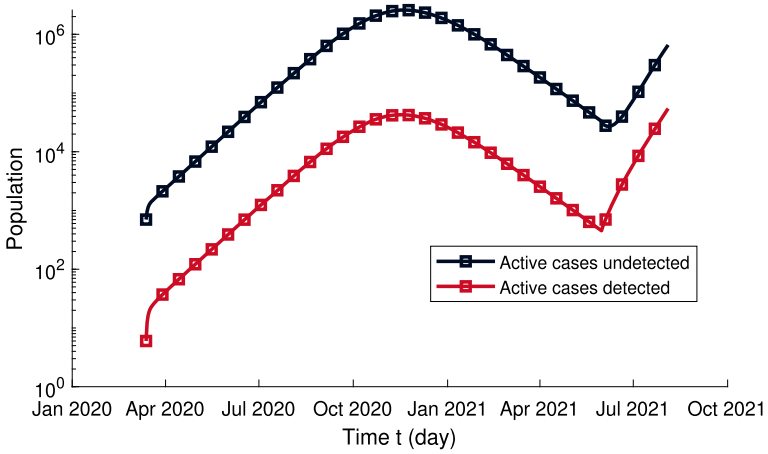


**Fig. 9** The predicted detected ($I_d$) and undetected ($I_u$) active cases in Morocco from March 13, 2020 to August 04, 2021

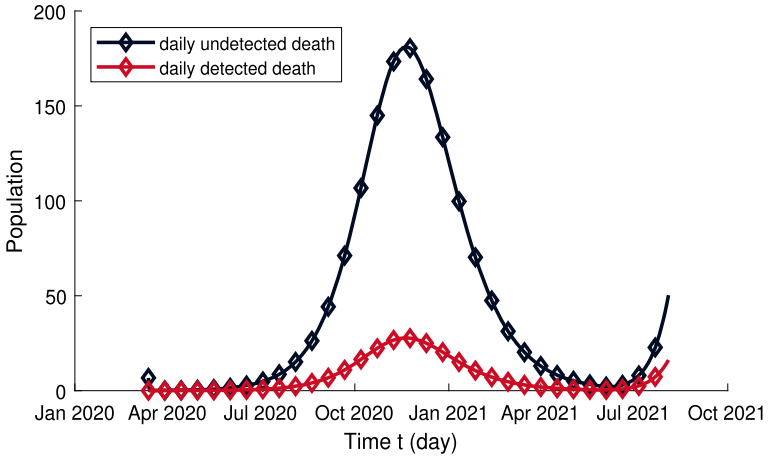


**Fig. 10** The predicted detected ($D_d$) and undetected ($D_u$) deaths not buried in Morocco from March 13, 2020 to August 04, 2021

The first scenario is when the transmission rate of infection from undetected cases changes by 50% (increases or decreases): in this case, the infection cases are expected to reach between 1,368,970 and 1,416,720, while the confirmed deaths will range between 18,628 and 19,243 cases, see Figs. 14, 15 and 16.

The second scenario is when the transmission rate of infection from detected cases changes by 50%: in this case, it is expected that the infection cases will reach between 1,134,019 and 1,457,895, while the confirmed deaths will range between 15,797 and 19,774 cases, see Figs. 17, 18 and 19.

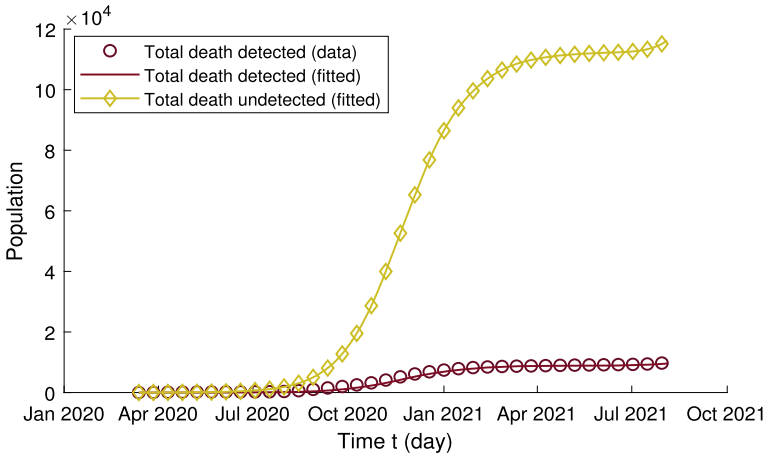


**Fig. 11** The predicted total deaths detected ($B_{\mathrm{d}}$) and undetected ($B_{\mathrm{u}}$) compared with real data of total deaths in Morocco from March 13, 2020 to August 04, 2021

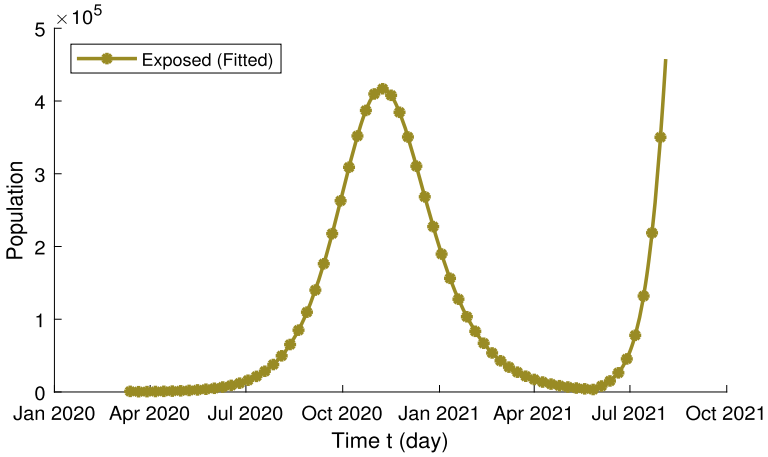


**Fig. 12** The predicted exposed (E) cases in Morocco from March 13, 2020 to August 04, 2021

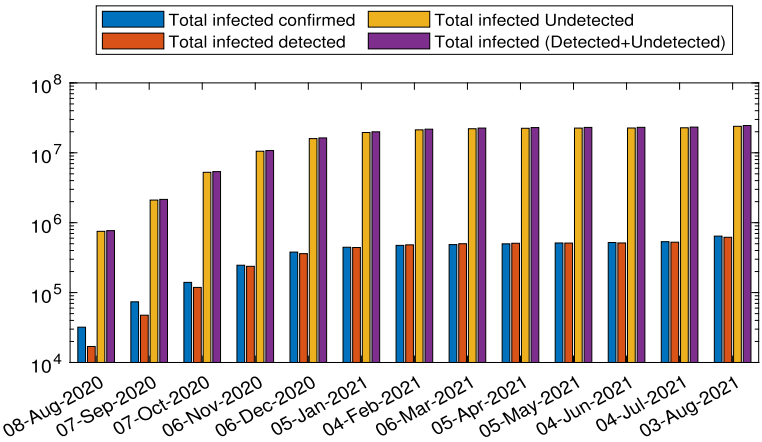


**Fig. 13** Bar graph of the comparison between confirmed cumulative cases, predicted detected and undetected cumulative cases, and total cumulative cases (detected + undetected) in Morocco from August 8, 2020 to August 3, 2021

**Table 4** The comparison between the number of detected and undetected (unreported) cases per month of COVID-19 in Morocco predicted by the proposed model

| Months | Detected | | | Undetected | | |
|---|---|---|---|---|---|---|
| | Infected | Recovered | Deaths | Infected | Recovered | Deaths |
| Mar. 2020 | 617 | 24 | 36 | 4413 | 2115 | 19 |
| Apr. 2020 | 4423 | 984 | 170 | 17,846 | 10,975 | 63 |
| May 2020 | 7783 | 7783 | 204 | 60,242 | 38,945 | 201 |
| Jun. 2020 | 12,385 | 8839 | 225 | 184,038 | 120,782 | 607 |
| Jul. 2020 | 24,322 | 17,658 | 353 | 566,193 | 374,980 | 1866 |
| Aug. 2020 | 62 590 | 47,595 | 1141 | 1 668,586 | 1,121,957 | 5567 |
| Sep. 2020 | 123,653 | 102,715 | 2194 | 4,315,324 | 3,005,364 | 14,912 |
| Oct. 2020 | 219,084 | 181,275 | 3695 | 9,370,023 | 7,027,960 | 34,907 |
| Nov. 2020 | 356,336 | 305,291 | 5846 | 14,989,878 | 12,409,454 | 61,732 |
| Dec. 2020 | 439,193 | 407,504 | 7388 | 19,064,015 | 17,231,028 | 85,829 |
| Jan. 2021 | 449,160 | 471,157 | 8275 | 21,124,734 | 20,116,664 | 100,276 |
| Feb. 2021 | 483,654 | 469,046 | 8623 | 21,972,580 | 21,421,616 | 106,815 |
| Mar. 2021 | 496,097 | 483,363 | 8818 | 22,384,736 | 22,085,314 | 110,142 |
| Apr. 2021 | 511,249 | 497,621 | 9023 | 22,550,749 | 22,358,527 | 111,511 |
| May 2021 | 519,216 | 519,216 | 9147 | 22,619,030 | 22,471,916 | 112,080 |
| Jun. 2021 | 531,361 | 517,576 | 9296 | 22,745,331 | 22,561,584 | 112,567 |
| Jul. 2021 | 623,528 | 561,930 | 9785 | 23,704,458 | 23,068,208 | 115,321 |

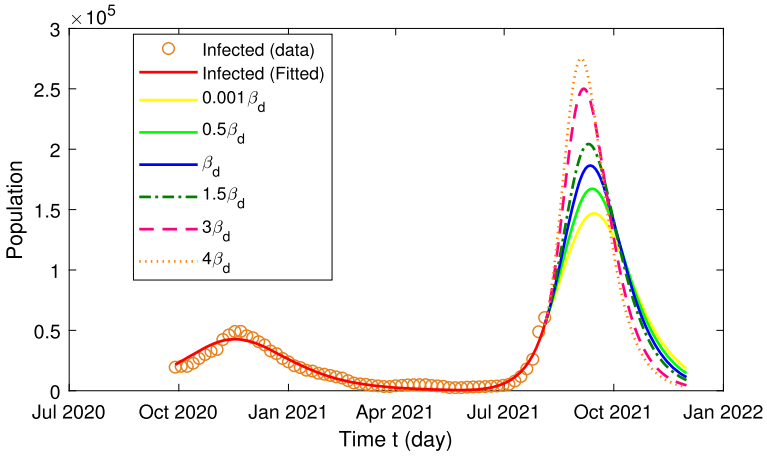


**Fig. 14** Different scenarios for the infected active cases detected ($I_d$) according to various values of transmission rate $\beta_d$ in Morocco after August 4, 2021

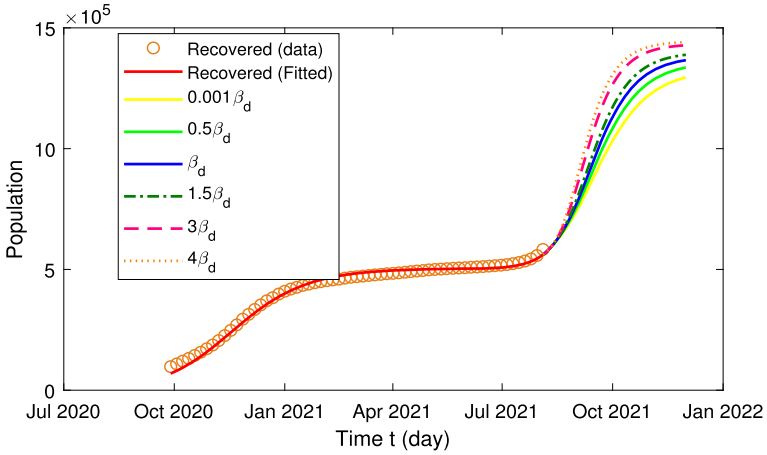


**Fig. 15** Different scenarios for the cumulative recovered detected cases ($R_d$) according to various values of transmission rate $\beta_d$ in Morocco after August 4, 2021

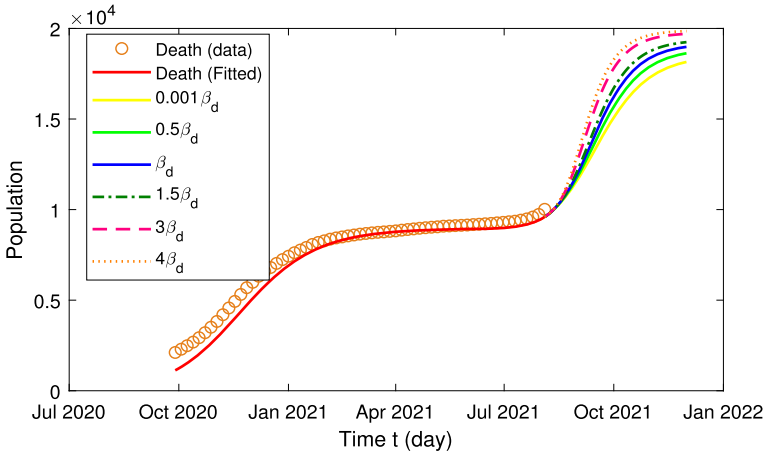


**Fig. 16** Different scenarios for the cumulative deaths detected cases ($B_d$) according to various values of transmission rate $\beta_d$ in Morocco after August 4, 2021

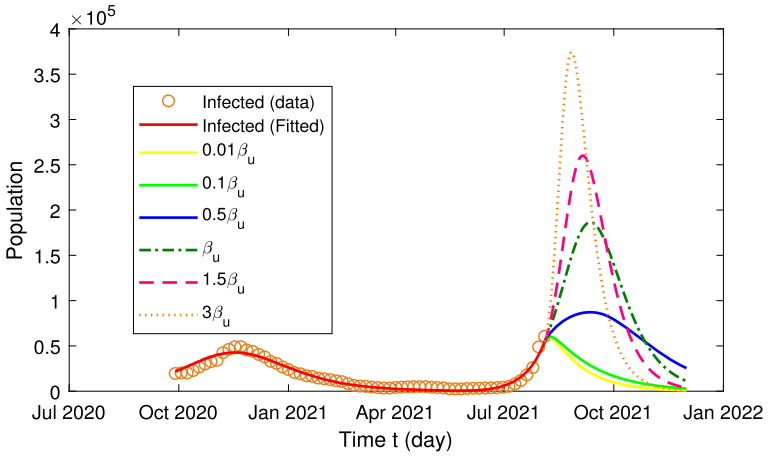


**Fig. 17** Different scenarios for the infected active cases detected ($I_d$) according to various values of transmission rate $\beta_u$ in Morocco after August 4, 2021

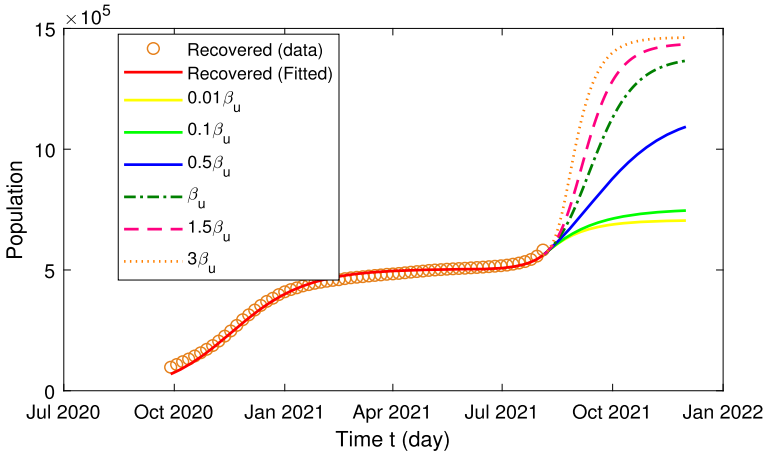


**Fig. 18** Different scenarios for the cumulative recovered cases detected ($R_d$) according to various values of transmission rate $\beta_u$ in Morocco after August 4, 2021

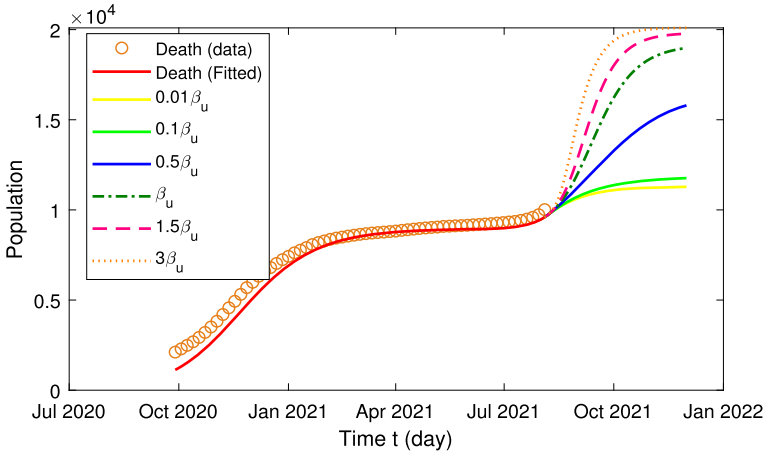


**Fig. 19** Different scenarios for the cumulative deaths cases detected ($B_d$) according to various values of transmission rate $\beta_u$ in Morocco after August 4, 2021

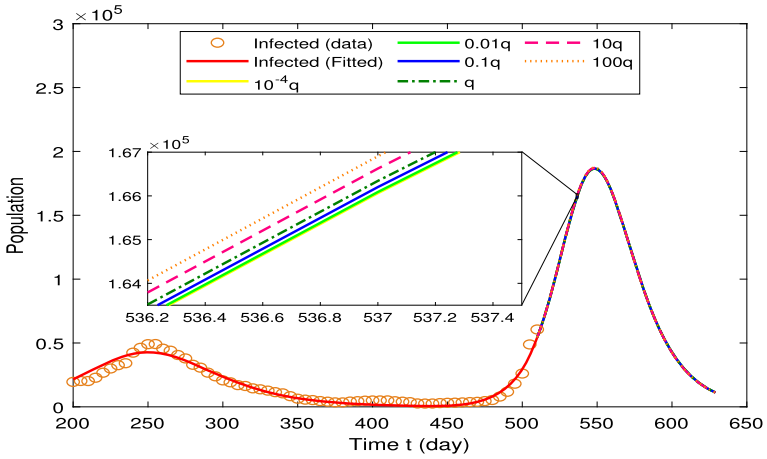


**Fig. 20** Different scenarios for the infected active cases detected ($I_d$) according to various values of transmission rate $q$ in Morocco after August 4, 2021

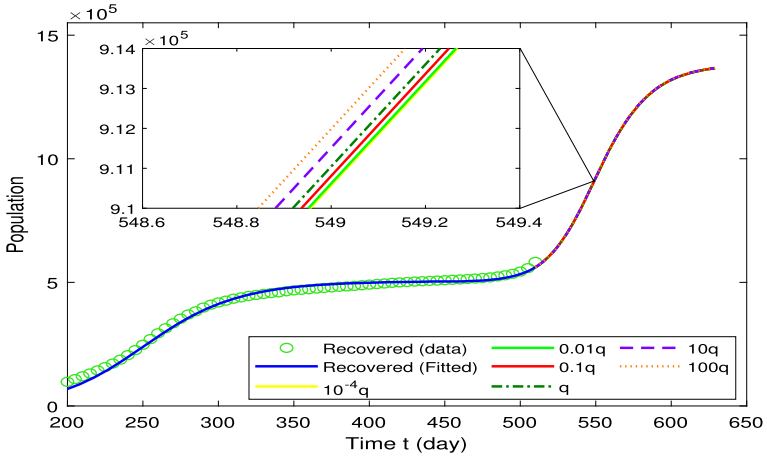


**Fig. 21** Different scenarios for the cumulative recovered ($R_d$) cases detected according to various values of transmission rate $q$ in Morocco after August 4, 2021

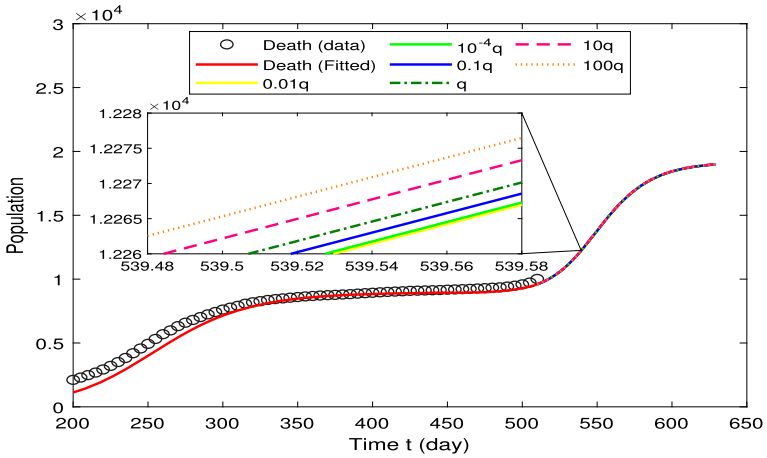


**Fig. 22** Different scenarios for the cumulative deaths cases detected ($B_d$) according to various values of transmission rate $q$ in Morocco after August 4, 2021

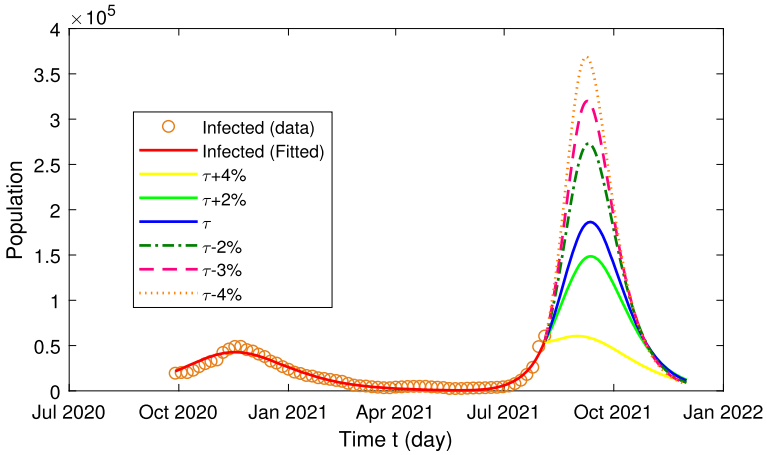


**Fig. 23** Different scenarios for the infected active cases detected ($I_d$) according to various values of $\tau$ in Morocco after August 4, 2021

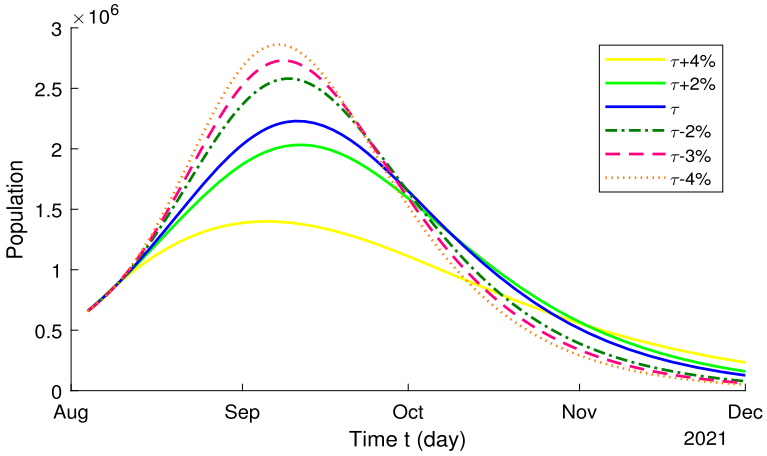


**Fig. 24** Different scenarios for the infected undetected active cases detected ($I_d$) according to various values of $\tau$ in Morocco after August 4, 2021

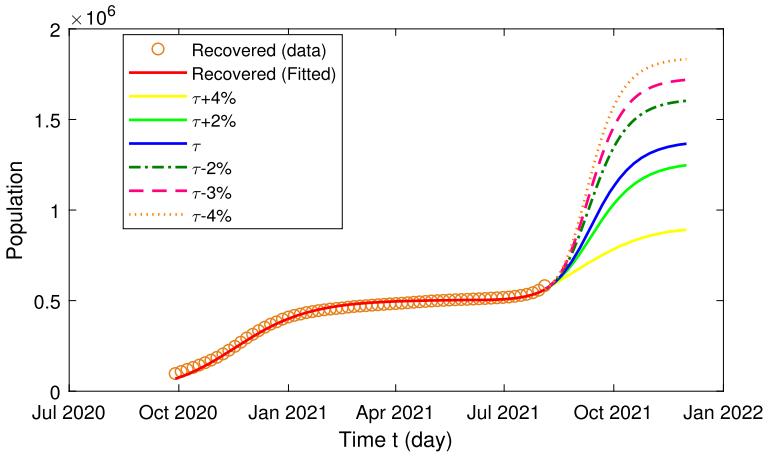


**Fig. 25** Different scenarios for the cumulative recovered cases detected ($R_d$) according to various values of $\tau$ in Morocco after August 4, 2021

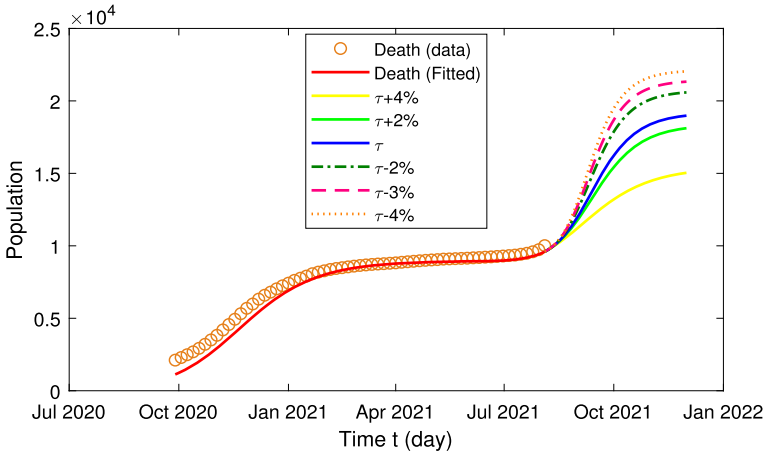


**Fig. 26** Different scenarios for the cumulative deaths cases detected ($B_{\mathrm{d}}$) according to various values of $\tau$ in Morocco after August 4, 2021

## 8 Conclusion

In this article, we have proposed an epidemiological model to predict the number of undetected cases of COVID-19 in Morocco, and this model can be easily applied to data from other countries, and this work shows that transmission of the virus does not occur. not only between susceptible and confirmed cases, but there are several infected cases due to contact with undetected cases, who in turn do not know they are carriers of the virus, which is the reason for the difficulty that the government finds to control virus.

The results of the parameters obtained are based on the constraints used, i.e., the intervals used for the parameters, in the case of Morocco, since this model is applied for the first time to the data of Morocco (for COVID-19) then the parameters must be estimated except the duration of infection for undetected infected $1/\gamma_{\mathrm{u}}$ which fixed at 14 according to the reference (Mahajan et al. 2021), the results can be improved if we add other data, but for our case we used the possible data and published on the internet. Otherwise, this model can be used for other countries and other diseases not just COVID-19.

Our approach gives a good approximation of the actual COVID-19 data from Morocco and will be used to estimate the undetected cases of COVID-19 in other countries of the world and to study other pandemics that have the same nature of spread as COVID-19. Some scenarios for the future days are discussed and presented graphically, this study allowed the government to choose a good control method such as isolation, quarantine, vaccination and to look for other method that would reduce contact between individuals such as distancing, masks, etc. Several studies can be followed for this work, for example using the optimal control of infected cases, or adding the age of the population or the different vaccines or variants of COVID-19. The studied model can be improved by invoking other effects, for example the number of tests, mobility, the presence of confinement, vaccination, etc.

## References


Alla Hamou A, Azroul EH, Hammouch Z, Alaoui AL (2020) A fractional multi-order model to predict the COVID-19 outbreak in Morocco. Appl Comput Math 20(1):177–203

Al-Salti N, Al-Musalhi F, ELmojtaba I, Gandhi V (2021) Sir model with time-varying contact rate. Int J Biomath 14(04):2150017

Barati R (2011) Parameter estimation of nonlinear Muskingum models using Nelder–Mead simplex algorithm. J Hydrol Eng 16(11):946–954

Brauer F, Castillo-Chavez C, Castillo-Chavez C (2012) Mathematical models in population biology and epidemiology, vol 2. Springer, Berlin

Burial rites in Morocco see drastic changes amid coronavirus outbreak. https://en.yabiladi.com/articles/details/91306/burial-rites-morocco-drastic-changes.html. Accessed July 2022

Calafiore GC, Novara C, Possieri C (2020) A modified SIR model for the COVID-19 contagion in Italy. In: 2020 59th IEEE conference on decision and control (CDC). IEEE, pp 3889–3894

Cohen J, Normile D (2020) New SARS-like virus in China triggers alarm. Science 367(6475):234–235. https://doi.org/10.1126/science.367.6475.234. ISSN:0036-8075

Da Silva A (2021) Modeling COVID-19 in Cape Verde Islands—an application of sir model. Comput Math Biophys 9(1):1–13

de Barros LC, Lopes MM, Pedro FS, Esmi E, dos Santos JPC, Sánchez DE (2021) The memory effect on fractional calculus: an application in the spread of COVID-19. Comput Appl Math 40(3):1–21

Deb K (2014) Multi-objective optimization. In: Search methodologies. Springer, Berlin, pp 403–449

Fuh C-C, Tsai H-H (2019) Parameter identification using the Nelder–Mead simplex algorithm for low signal-to-noise ratio systems in a frequency domain. J Mar Sci Technol 27(4):4

Gabbrielli M, Gandolfo C, Anichini G, Candelori T, Benvenuti M, Savellini GG, Cusi MG (2021) How long can SARS-CoV-2 persist in human corpses? Int J Infect Dis 106:1–2. https://doi.org/10.1016/j.ijid.2021.03.052. ISSN:1201-9712

Gao D, Lou Y, He D, Porco TC, Kuang Y, Chowell G, Ruan S (2016) Prevention and control of Zika as a mosquito-borne and sexually transmitted disease: a mathematical modeling analysis. Sci Rep 6(1):1–10

Gunantara N (2018) A review of multi-objective optimization: methods and its applications. Cogent Eng 5(1):1502242. https://doi.org/10.1080/23311916.2018.1502242

Hal LS (1995) An introduction to the theory of competitive and cooperative systems. Mathematical surveys and monographs, vol 41

Hamou AA, Azroul E, Hammouch Z et al (2021a) On dynamics of fractional incommensurate model of Covid-19 with nonlinear saturated incidence rate. medRxiv

Hamou AA, Azroul E, Alaoui AL (2021b) Fractional model and numerical algorithms for predicting COVID-19 with isolation and quarantine strategies. Int J Appl Comput Math 7(4):1–30

Haque TS, Alam S, Chakraborty A (2022) Selection of most effective COVID-19 virus protector using a novel MCGDM technique under linguistic generalised spherical fuzzy environment. Comput Appl Math 41(2):1–23

Huo X, Chen J, Ruan S (2021) Estimating asymptomatic, undetected and total cases for the COVID-19 outbreak in Wuhan: a mathematical modeling study. BMC Infect Dis 21(1):1–18

Ivorra B, Ferrández MR, Vela-Pérez M, Ramos AM (2020) Mathematical modeling of the spread of the coronavirus disease 2019 (COVID-19) taking into account the undetected infections. the case of China. Commun Nonlinear Sci Numer Simul 88:105303

Korobeinikov A (2009) Global properties of SIR and SEIR epidemic models with multiple parallel infectious stages. Bull Math Biol 71(1):75–83

Korobeinikov A, Wake GC (2002) Lyapunov functions and global stability for sir, sirs, and sis epidemiological models. Appl Math Lett 15(8):955–960

Lagarias JC, Reeds JA, Wright MH, Wright PE (1998) Convergence properties of the Nelder–Mead simplex method in low dimensions. SIAM J Optim 9(1):112–147

Li R, Pei S, Chen B, Song Y, Zhang T, Yang W, Shaman J (2020) Substantial undocumented infection facilitates the rapid dissemination of novel coronavirus (SARS-CoV-2). Science 368(6490):489–493. https://doi.org/10.1126/science.abb3221

Liu X, Stechlinski P (2012) Infectious disease models with time-varying parameters and general nonlinear incidence rate. Appl Math Model 36(5):1974–1994. https://doi.org/10.1016/j.apm.2011.08.019. ISSN:0307-904X

Ma Z (2009) Dynamical modeling and analysis of epidemics. World Scientific, Singapore

Mahajan A, Sivadas NA, Solanki R (2020) An epidemic model SIPHERD and its application for prediction of the spread of COVID-19 infection in India. Chaos Solitons Fractals 140:110156

Mahajan A, Solanki R, Sivadas N (2021) Estimation of undetected symptomatic and asymptomatic cases of COVID-19 infection and prediction of its spread in the USA. J Med Virol 93(5):3202–3210
Pei S, Kandula S, Yang W, Shaman J (2018) Forecasting the spatial transmission of influenza in the United States. Proc Natl Acad Sci 115(11):2752–2757. https://doi.org/10.1073/pnas.1708856115
Perakis G, Singhvi D, Lami OS, Thayaparan L (2022) COVID-19: a multiwave SIR-based model for learning waves. Prod Oper Manag
Procedures adopted during the burial of the dead in Corona in Morocco. https://ar.le360.ma/societe/163357. Accessed July 2022
Ram V, Schaposnik LP (2021) A modified age-structured SIR model for COVID-19 type viruses. Sci Rep 11(1):1–15
Rippinger C, Bicher M, Urach C, Brunmeir D, Weibrecht N, Zauner G, Sroczynski G, Jahn B, Mühlberger N, Siebert U et al (2021) Evaluation of undetected cases during the COVID-19 epidemic in Austria. BMC Infect Dis 21(1):1–11
Salje H, Kiem CT, Lefrancq N, Courtejoie N, Bosetti P, Paireau J, Andronico A, Hozé N, Richet J, Dubost C-L, Le Strat Y, Lessler J, Levy-Bruhl D, Fontanet A, Opatowski L, Boelle P-Y, Cauchemez S (2020) Estimating the burden of SARS-CoV-2 in France. Science 369(6500):208–211. https://doi.org/10.1126/science.abc3517
Simoy MI, Aparicio JP (2022) Socially structured model for COVID-19 pandemic: design and evaluation of control measures. Comput Appl Math 41(1):1–22
Sriwijitalai W, Wiwanitkit V (2020) COVID-19 in forensic medicine unit personnel: observation from Thailand. J Forensic Leg Med 72:101964. https://doi.org/10.1016/j.jflm.2020.101964. ISSN:1752-928X
Toda AA (2020) Susceptible-infected-recovered (SIR) dynamics of COVID-19 and economic impact1. Covid Econ 43
Watson J, Whiting PF, Brush JE (2020) Interpreting a covid-19 test result. BMJ 369
Watve M, Bhisikar H, Kharate R (2021) Epidemiology: gray immunity model gives qualitatively different predictions
Worldometer (2020) International team of developers, researchers and volunteers. https://www.worldometers.info/world-population. Accessed 5 July 2020
Worldometers (2020a) Coronavirus incubation period. https://www.worldometers.info/coronavirus/coronavirus-incubation-period/. Accessed 17 Sept 2020
Worldometers (2020b) Morocco population. https://www.worldometers.info/world-population/morocco-population/. Accessed 17 Sept 2020
Yaacoub S, Schünemann HJ, Khabsa J, El-Harakeh A, Khamis AM, Chamseddine F, El Khoury R, Saad Z, Hneiny L, Garcia CC, Muti-Schünemann GEU, Bognanni A, Chen C, Chen G, Zhang Y, Zhao H, Hanna PA, Loeb M, Piggott T, Reinap M, Rizk N, Stalteri R, Duda S, Solo K, Chu DK, Akl EA (2020) Safe management of bodies of deceased persons with suspected or confirmed COVID-19: a rapid systematic review. BMJ Glob Health. https://doi.org/10.1136/bmjgh-2020-002650
Yang X-S (2014) Chapter 14—Multi-objective optimization. In: Yang X-S (ed) Nature-inspired optimization algorithms. Elsevier, Oxford, pp 197–211. https://doi.org/10.1016/B978-0-12-416743-8.00014-2. ISBN:978-0-12-416743-8
Yang HM, Junior LPL, Castro FFM, Yang AC (2021) Evaluating the impacts of relaxation and mutation in the SARS-CoV-2 on the COVID-19 epidemic based on a mathematical model: a case study of São Paulo state (Brazil). Comput Appl Math 40(8):1–27
Zapor M (2020) Persistent detection and infectious potential of SARS-CoV-2 virus in clinical specimens from COVID-19 patients. Viruses 12(12). https://doi.org/10.3390/v12121384. https://www.mdpi.com/1999-4915/12/12/1384
Zhu H, Zhang H, Ni S, Korabečná M, Yobas L, Neuzil P (2020) The vision of point-of-care PCR tests for the COVID-19 pandemic and beyond. TrAC Trends Anal Chem 130:115984